

Isolation, characterization and applications of nanocellulose produced by ancestral enzymes

Borja Alonso Lerma
PhD Thesis

eman ta zabal zazu



Universidad Euskal Herriko
del País Vasco Unibertsitatea

Donostia, 2019

**EUSKAL HERRIKO UNIBERTSITATEA - UNIVERSIDAD DEL PAIS VASCO
PHYSICS OF NANOSTRUCTURES AND ADVANCED MATERIALS -
FÍSICA DE NANOESTRUCTURAS Y MATERIALES AVANZADOS**



GIPUZKOAKO
INGENIARITZA
ESKOLA
ESCUELA
DE INGENIERÍA
DE GIPUZKOÁ

Isolation, characterization and applications of nanocellulose produced by ancestral enzymes

Borja Alonso Lerma
PhD Thesis

Thesis supervisors:
Dr. Raul Perez Jimenez
Dr. M^a Aranzazu Eceiza Mendiguren

Donostia, 2019

Acknowledgment

En primer lugar me gustaría agradecer a mis directores de tesis, al Dr. Raul Perez Jimenez, jefe del grupo de Nanobiomecánica en CIC nanoGune por darme la oportunidad de unirme a su grupo y permitirme empezar este trabajo bajo su supervisión durante estos años. A la Dr. Arantxa Eceiza, jefa del Grupo de Materiales + Tecnologías (GMT) del Departamento de Ingeniería Química y del Medio ambiente de la UPV/EHU por unirse a este proyecto y su apoyo para llevar esta tesis a buen término. Además de a CIC nanoGune, a la UPV/EHU y al Gobierno Vasco por haber financiado este trabajo.

Me gustaría agradecer a los Servicios Generales (SGIker) de la UPV/EHU por el apoyo técnico durante esta tesis. En especial a los a las unidades de Macroconducta, Mesoestructura y Nanotecnología, de Rayos X y de Resonancia Magnética Nuclear. Además de al Dr. Iban Amenabar (CIC nanoGune) por sus medidas de nano-FTIR.

Igualmente, me gustaría agradecer a todos mis compañeros que han pasado por el grupo de Nanobiomechanica de CIC nanoGune durante estos años por su ayuda, los buenos momentos y apoyo. Sobre todo a Leire por estar siempre ahí cuando lo he necesitado y a mis andaluces, Ana y Antonio.

Además agradecer a mis compañeros del GMT del Departamento de Ingeniería Química y del Medio Ambiente de la UPV/EHU, en especial a Lorena e Izaskun, por ayudarme a realizar este trabajo.

Por último a mi familia y amigos por estar siempre ahí. Aunque estemos lejos siempre me habéis apoyado para continuar este camino. Sobre todo agradecer a mis padres y a mis hermanos por todo.

Table of content

Summary	1
Resumen	3
Chapter I: Introduction	9
Objectives	35
Chapter II: Materials and methods	39
2.1 Reactants	40
2.2 Protein expression and purification	40
2.2.1 Ancestral Endoglucanases expression	42
2.2.2 Cloning of the ANC EG gene to the CBM from <i>B. subtilis</i> EG	43
2.2.2.1 Commercial plasmid amplification with the CBM gene	44
2.2.2.2 Digestion of commercial plasmid with CBM gene and pQE-80L with ANC EG gene	44
2.2.2.3 Ligation of pQE-80L+ANC EG with CBM from <i>B. subtilis</i> EG	45
2.2.2.4 pQE-80L+ANC EG+CBM amplification	46
2.2.2.5 Expression test of ANC EG+CBM	46

2.2.2.6 Protein production and purification of ANC EG+CBM	47
2.2.3 Protein production and purification of <i>Thermotoga maritima</i> and <i>Bacillus subtilis</i> EGs	47
2.2.4 Protein production and purification of ancestral and <i>B. subtilis</i> xylanases	47
2.2.5 Protein production and purification of ancestral and <i>Streptomyces viridosporus</i> LPMOs	49
2.3 Enzymatic nanocellulose isolation	49
2.3.1 From filter paper	49
2.3.2 From lignocellulose complex substrates	50
2.3.3 Nanocellulose and reducing sugar yields	52
2.4 Nanocellulose characterization	53
2.4.1 Atomic force microscopy	53
2.4.2 Fourier-transform infrared spectroscopy	54
2.4.3 Nanoscale-resolved Fourier transforms infrared spectroscopy	55
2.4.4 Sulfur content calculation by conductometric titration	56
2.4.5 X-Ray diffraction	57
2.4.6 Solid-state cross-polarization magic angle spinning	58

¹³ C nuclear magnetic resonance	
2.4.7 Thermogravimetric analysis	60
2.5 WBPU/CNC nanocomposites	61
2.5.1 Preparation of waterborne polyurethane (WBPU)	61
2.5.2 WBPU/CNC nanocomposites	62
2.5.3 Dynamic light scattering	64
2.5.4 AFM	64
2.5.5 FTIR	65
2.5.6 Differential scanning calorimetry	65
2.5.7 TGA	66
2.5.8 Dynamic mechanical analysis	67
2.5.9 Mechanical test	67
2.5.10 Water contact angle	68
2.6 Conductive nanopapers	69
2.6.1 CNC nanopapers films	69
2.6.2 CNC/graphene nanopapers films	69
2.6.3 AFM of graphene sheets	70
2.6.4 Mechanical properties	71

2.6.5 WCA	71
2.6.6 TGA	71
2.6.7 FTIR	72
2.6.9 Scanning electron microscopy	72
2.6.10 Electrical conductivity measurement	72
2.6.11 CVD graphene deposition in nanocellulose film	73
Chapter III: Nanocellulose isolation with ancestral endoglucanase	77
3.1 Isolation of nanocellulose from filter paper	78
3.2 Nanocellulose yield by enzymatic hydrolysis	80
3.3 Characterization of nanocellulose	83
3.3.1 Morphology	83
3.3.2 Physicochemical characterization	90
3.3.2.1 Chemical structure by FTIR	90
3.3.2.2 Chemical structure of individual particles by IR s-SNOM and nano-FTIR	97
3.3.2.3 Sulfur content determination by conductometric titration	99
3.3.2.4 Crystalline structure of nanocellulose by XRD	101
3.3.2.5. Chemical structure of nanocellulose by CP/MAS	105

¹³ C NMR	
3.3.2.6 Thermal stability of nanocellulose by TGA	107
Chapter IV: Nanocellulose isolation from lignocellulosic biomass with enzymatic cocktail	113
4.1 Nanocellulose isolation from lignocellulosic materials	114
4.2 Nanocellulose yield by enzymatic hydrolysis	115
4.3 Characterization of nanocellulose	118
4.3.1 Morphology	118
4.3.2 Physicochemical characterization	122
4.3.2.1 Chemical structure by FTIR	122
4.3.2.2 Crystalline structure of nanocellulose by XRD	129
4.3.2.3. Chemical structure of nanocellulose by CP/MAS	132
¹³ C NMR	
4.3.2.4 Thermal stability of nanocellulose by TGA	135
Chapter V: Enzymatic nanocellulose applications	141
5.1 Waterborne polyurethane/CNC films	142
5.1.1 Film appearance	143
5.1.2 Morphology	144
5.1.3 SEM images of cross section	146

5.1.4 Physicochemical properties	147
5.1.5 Thermal properties	152
5.1.6 Thermal stability	156
5.1.7 Thermomechanical properties	160
5.1.8 Mechanical properties	164
5.1.9 Hydrophobicity	167
5.2 Graphene and nanocellulose films	169
5.2.1 CNC film fabrication	169
5.2.2 Graphene-CNC films	172
5.2.3 Morphological analysis	173
5.2.4 Physicochemical analysis	175
5.2.5 Mechanical properties	178
5.2.6 Thermal properties	181
5.2.7 Hydrophobicity	183
5.2.8 Conductive properties	184
5.2.9 EnCNC film + graphene CVD	186
Chapter VI: Discussion	191
Future works	202

Bibliography	205
Annexes	233
List of Figures	231
List of Tables	243
List of Abbreviations	246
List of Symbols	250

Summary

Efficient, controlled and sustainable nanocellulose isolation is still a challenge with current methodologies. Enzyme hydrolysis shows up as a novel alternative, but yields are lower in comparison with chemical methods. To improve this process, we need new enzymes with higher performances. Here we propose the use of ancestral enzymes developed with ancestral sequence reconstruction (ASR); these had shown higher activity, stability and promiscuity than the extant ones, matching them ideally for biotechnology application. Here, we propose a method to produce high pure nanocellulose by ancestral endoglucanase hydrolysis. This method allows controlling nanocellulose size and maintains the native cellulose structure where the chemical or mechanical methods fail. This enzymatic nanocellulose shows higher crystallinity and thermostability than a commercial nanocellulose sample produced by acid sulfuric treatment.

The optimized protocol was used to isolate nanocellulose from lignocellulosic substrates. In this case we used treatments with addition of different ancestral enzymes as xylanase and lytic polysaccharide monooxygenase (LPMO), to help ancestral endoglucanase hydrolysis. We achieved nanocellulose isolation from two lignocellulosic pulps with different properties. Also, we observed how LPMO produced nanocellulose oxidation. Here, we propose LPMO as substitution of chemical oxidation of cellulose, demonstrating that the enzymatic method can substitute both nanocellulose isolation and modification by chemical methods.

The enzymatic nanocellulose can be used in high performance tailored materials. In this work we studied our nanocellulose in two different applications. The first one was as reinforcement for thermoplastic materials, in our case waterborne polyurethane (WBPU). As control we used commercial nanocellulose produced by sulfuric acid. We observed that small nanocellulose addition produced nanocomposites with higher thermal and mechanical properties, and nanocomposites with our nanocellulose had better properties than the ones prepared with the acid hydrolyzed nanocellulose. Moreover, we introduced the enzymatic nanocellulose to manufacture conductive nanopapers with graphene addition by two different strategies. We produced nanopapers with high thermal, mechanical and conductive properties by mixing enzymatic nanocellulose with different concentration of reduced graphene. Moreover, by graphene chemical vapor deposition (CVD) over a nanocellulose film we manufactured transparent conductive films, as substitution of plastic or metal substrates.

Resumen

El principal objetivo de esta tesis ha sido desarrollar y optimizar un método para el aislamiento de nanocelulosa basado en el uso de enzimas ancestrales y estudiar sus posibles aplicaciones. La nanocelulosa es un nuevo biomaterial que ha atraído la atención de la comunidad científica debido a sus extraordinarias cualidades como tamaño nanométrico, flexibilidad, o sus propiedades mecánicas, térmicas y eléctricas. Además es un material biocompatible y sostenible. Estas partículas se pueden organizar según su tamaño, cristalinidad y su origen: los nanocristales de celulosa (CNC) son pequeñas partículas cristalinas con longitudes entre 50 a 1000 nm. Las nanofibras de celulosa (CNFs) son fibras nanométricas de varias micras y contienen regiones amorfas y cristalinas en su estructura. Además, existe un grupo de bacterias capaces de secretar nanofibras de celulosa como ocurre con la celulosa bacteriana (BC).

Existen diferentes métodos para el aislamiento de nanocelulosa: mecánicos, químicos y enzimáticos. El proceso mecánico consiste en diferentes pasos de homogenización a alta presión que permiten la obtención de CNFs. Normalmente es combinado con tratamientos químicos o enzimático para mejorar el rendimiento y reducir el consumo energético. El método químico es el más utilizado, concretamente el tratamiento con ácido sulfúrico. Este ácido es capaz de degradar las regiones amorfas de la celulosa y mantener los dominios cristalinos, pero presenta algunos inconvenientes. Durante el proceso se generan grandes cantidades de residuos tóxicos como las aguas residuales generadas

durante los pasos de neutralización y diálisis. Se producen reacciones de esterificación en la superficie de los cristales sustituyendo los grupos hidroxilos por grupos sulfatos, modificando las propiedades fisicoquímicas y dificultando el secado del material por la gran hidrofiliidad de estos grupos.

Es por todo ello que se necesitan nuevos métodos que mejoren los actuales para producir nanocelulosa de manera eficiente, sostenible y controlada. Las enzimas lignocelulosicas, capaces de degradar la biomasa, son una de las alternativas más prometedoras, sin embargo para su implementación necesitamos enzimas con mayor actividad y promiscuidad. En esta tesis hemos propuesto el empleo de enzimas ancestrales desarrolladas con técnicas de reconstrucción de secuencias ancestrales (ASR). Estas enzimas han demostrado tener mayor actividad, promiscuidad y estabilidad que las enzimas actuales. En una tesis anterior desarrollada en el grupo de Nanobiomecánica (CIC nanoGune), realizamos la reconstrucción de una endoglucanasa, enzimas capaces de degradar celulosa, ancestral con 2.000 millones de años. Esta endoglucanasa ancestral (ANC EG) demostró mayor actividad y estabilidad en un amplio rango de pH y temperatura que las endoglucanasas modernas, además degradaban con mayor eficiencia sustratos como cartón. Esta ANC EG mostró las características ideales para su implementación en la producción de nanocelulosa.

En primer lugar nuestro objetivo fue la optimización del proceso de obtención de nanocelulosa y su posterior caracterización empleando la hidrólisis de la ANC EG sobre papel de filtro. Con la intención de mejorar la actividad catalítica en sustratos recalcitrantes, añadimos a la

ANC EG un dominio de unión a celulosa de la endoglucanasa de *Bacillus subtilis* (CBM), obteniendo la enzima quimérica ANC EG+CBM. En estos experimentos medimos una mayor conversión de nanocelulosa y azúcares reducidos durante la hidrólisis de ANC EG+CBM en comparación con la enzima con solo dominio catalítico, ANC EG. Además, ambas enzimas ancestrales demostraron mayor actividad que la endoglucanasa de *Thermotoga maritima* usada como control. Analizamos el tamaño y morfología de la nanocelulosa usando microscopía de fuerzas atómicas. Observamos que la hidrólisis a tiempos cortos producía fibras con morfología correspondientes a nanofibras. Al continuar la hidrólisis hasta 24 horas, el tamaño se reducía, apareciendo partículas similares a nanocristales. La población más homogénea de nanocristales se consiguió manteniendo la hidrólisis de ANC EG+CBM durante 24 horas.

Al comparar la morfología de los cristales producidos por hidrólisis enzimática (EnCNC) con una muestra comercial de nanocristales obtenidos por tratamiento con ácido sulfúrico (AcCNC) observamos diferencias. Los EnCNC mostraban aspecto de aguja, en cambio los AcCNC de cinta. Estas morfologías correspondían a diferentes polimorfos estructurales de celulosa. Los EnCNC mostraban la estructura nativa de celulosa, celulosa tipo I y AcCNC de la celulosa tipo II. Los EnCNC y AcCNC fueron caracterizados por diferentes técnicas fisicoquímicas. Con estos análisis confirmamos que EnCNC mantenían la estructura de celulosa tipo I, mientras que los AcCNC eran mezcla tipo I y tipo II, el tratamiento ácido transformaba parcialmente la estructura. La cristalinidad y estabilidad térmica de los EnCNC era mayor que los

AcCNC debido a la sustitución de los grupos hidróxilos por sulfatos en la superficie de los cristales y a que estos catalizan la degradación.

En la segunda parte de esta investigación decimos aislar nanocelulosa utilizando como sustrato dos materiales lignocelulosicos compuestos por todos los polímeros de la biomasa: celulosa, hemicelulosa y lignina. En este caso, realizamos tratamientos enzimáticos integrando otras enzimas ancestrales con diferentes actividades catalíticas, como xilanasas capaces de depolimerizar hemicelulosa, y monoxigenasas líticas de polisacáridos (LPMO) que degradan la celulosa por oxigenación. En estas hidrólisis se estudió el efecto de diferentes mezclas de estas enzimas, todas ellas incluyendo la ANC EG+CBM, en el rendimiento y las propiedades fisicoquímicas de las nanocelulosas obtenidas. Los rendimientos de nanocelulosa y azúcares reducidos aumentaban con la adición de xilanasas y LPMO debido a la actividad sinérgica de estas enzimas con ANC EG+CBM. La utilización de las tres enzimas en cocktail exhibió la mayor conversión de nanocelulosa en los dos sustratos. Además, comparamos la actividad de este cocktail ancestral con un cocktail de enzimas actuales, obteniendo mejores resultados con las enzimas ancestrales. Las nanocelulosas producidas desde estos sustratos mostraban, en general, mayor cristalinidad con la adición de xilanasas y LPMO, pero eran menores que las obtenidas en la nanocelulosa de papel de filtro, debido a la baja cristalinidad de los sustratos de partida. Las nanocelulosas mantenían estabilidades térmicas similares y tamaños menores.

Durante la caracterización de estas nanocelulosas, descubrimos que el empleo de LPMO resultaba en nanocelulosa oxidada. La nanocelulosa

oxidada generalmente es producida por tratamientos químicos y tiene una gran variedad de aplicaciones por su gran reactividad. La función de LPMO para la modificación de nanocelulosa no ha sido descrita previamente, ni su uso en la producción de nanocelulosa, siendo esta tesis uno de los primeros trabajos en demostrarlo. Además, demuestra que las enzimas ancestrales pueden sustituir los procedimientos químicos tanto en la producción como en la modificación de nanocelulosa.

Finalmente, quisimos estudiar distintas aplicaciones de nuestra EnCNC producida desde papel de filtro para demostrar su versatilidad y su implementación en aplicaciones de altas prestaciones. En primer lugar fue utilizada como refuerzo para materiales termoplásticos, concretamente poliuretanos en base de agua, y comparados a su vez con AcCNC. Observamos como pequeñas cantidades de nanocristales mejoraban las propiedades termomecánicas. Además, la adición de EnCNC aumentaba estas propiedades de manera más eficiente que los AcCNC en la misma concentración, manifestando como las propiedades fisicoquímicas de los nanocristales tienen un efecto en las propiedades del material final. En segundo lugar estudiamos la formación de nanopapeles conductores con EnCNC y grafeno, estos experimentos no pudieron compararse con AcCNC debido a la imposibilidad de éstos para formar nanopapeles estables. En este caso observamos como la adición de grafeno a la matriz de EnCNC resultaba en la fabricación de nanopapeles con elevadas propiedades mecánicas, conductoras y térmicas. Incluso, fabricamos nanopapeles conductores transparentes mediante deposición química en fase vapor de una mono capa de grafeno, proponiendo la nanocelulosa como sustrato en sustitución de materiales plásticos o metálico

Chapter I: Introduction

Cellulose is the most abundant renewable biopolymer on Earth and it is the main structural component of the lignocellulosic biomass. Cellulose is present not only in the cell wall of plants, but as a part of other organisms such as fungi [1], bacteria [2], algae [3] or animals like tunicates [4]. Cellulose is a linear homopolymer composed by D-glucose units bonded together by β -1,4-glycosidic bonds, where each unit is rotated 180° to the next one. The smallest unit that two D-glucose units form is named cellobiose, and it has a size of 1,03 nm (Figure 1.1). The polymerization degree of cellulose can oscillate depending on its source, in wood-derived cellulose is normally of 1000 glucose units, in cellulose from cotton is 10000 units, and in bacteria is around 500 units [5].

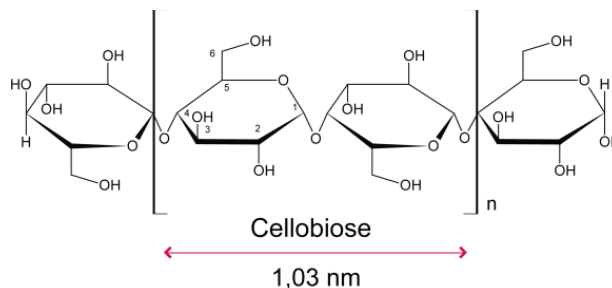


Figure 1.1. Cellulose chemical structure. Cellobiose is the repeating unit of the cellulose polymer and is formed by two D-glucose units bonded together by a β -1,4-glycosidic bond. Each unit is rotated 180° to the next and has three hydroxyl groups that made the polymer very reactive.

The D-glucose units have three hydroxyl groups that are responsible for some cellulose properties such as chirality, hydrophilicity, and biodegradability. The natural linear structure of cellulose and the number of hydroxyl groups help the formation of hydrogen bond that produces the ordered crystalline structure and provides the high mechanical properties to the fibers. The hydrogen bonds can be formed between different cellulose chains (intermolecular bond) or in the same chain (intramolecular bond) (Figure 1.2). The intramolecular bonding provides stiffness and the intermolecular bonding shapes the crystal structure. The high amount of hydrogen bonds and the crystallinity made the cellulose an insoluble material in water and in the majority of organic solvents [6].

Cellulose is a semi-crystalline polymer and is divided into crystalline and amorphous fractions. The crystalline domains are very packed together and are very difficult to degrade by chemical or enzymatic treatment. In the amorphous regions, the chains are disorganized and are easier to degrade [7]. The proportions between both domains depend on the cellulose source and the treatment used to extract the fibers [8].

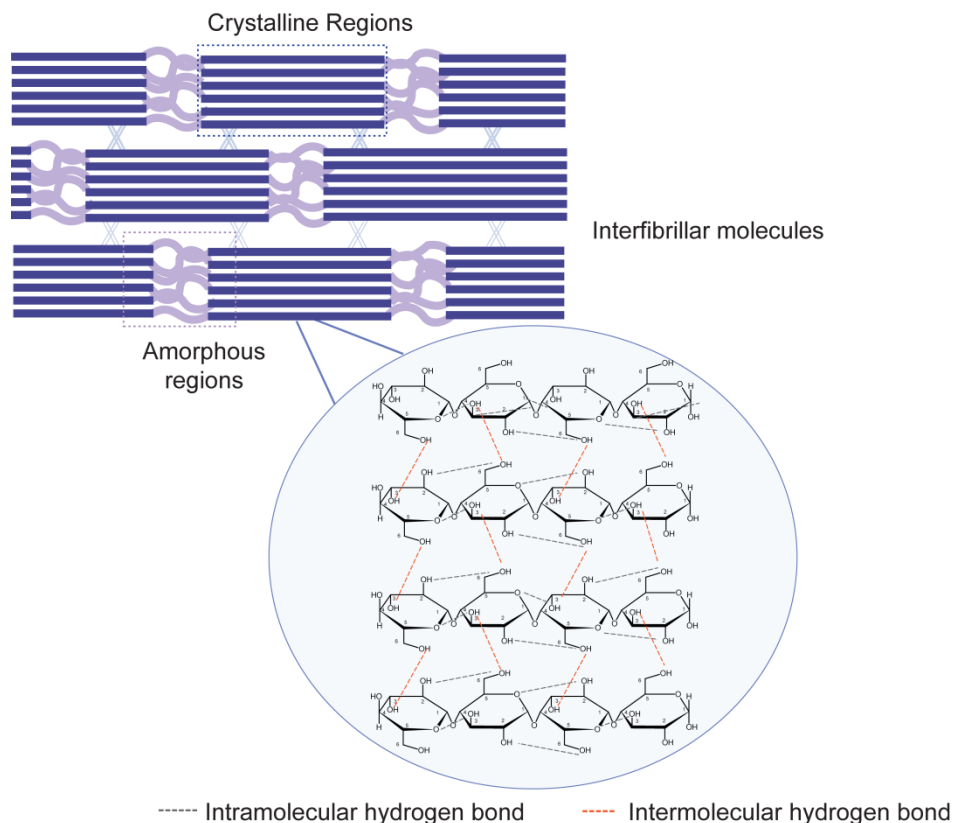


Figure 1.2. Cellulose semi-crystalline structure. Cellulose polymer is organized in crystalline regions, where the glucose chains are tied together by inter- and intramolecular hydrogen bonds producing a very recalcitrant structure, and an amorphous region where the chains are disorganized and are more accessible to degradation.

We can organize cellulose into polymorphs or allomorphs depending on the inter- and intramolecular hydrogen bonds and their molecular orientations. There are six polymorphs described in the literature: cellulose I, II, III_I, III_{II}, IV_I and IV_{II}. The native and most abundant form of cellulose is the type I, and all the polymorphs can be produced from it with different physicochemical treatments (Figure 1.3). Cellulose I has

the chains of the polymer in a parallel organization and it can be also organized in two polymorphs, cellulose I α and I β [9]. These two type I polymorphs can be found together, and the ratio between them vary with the cellulose source. The cellulose I α is abundant in algae and bacterial cellulose [10] and cellulose I β is more present in higher plants and tunicates [11].

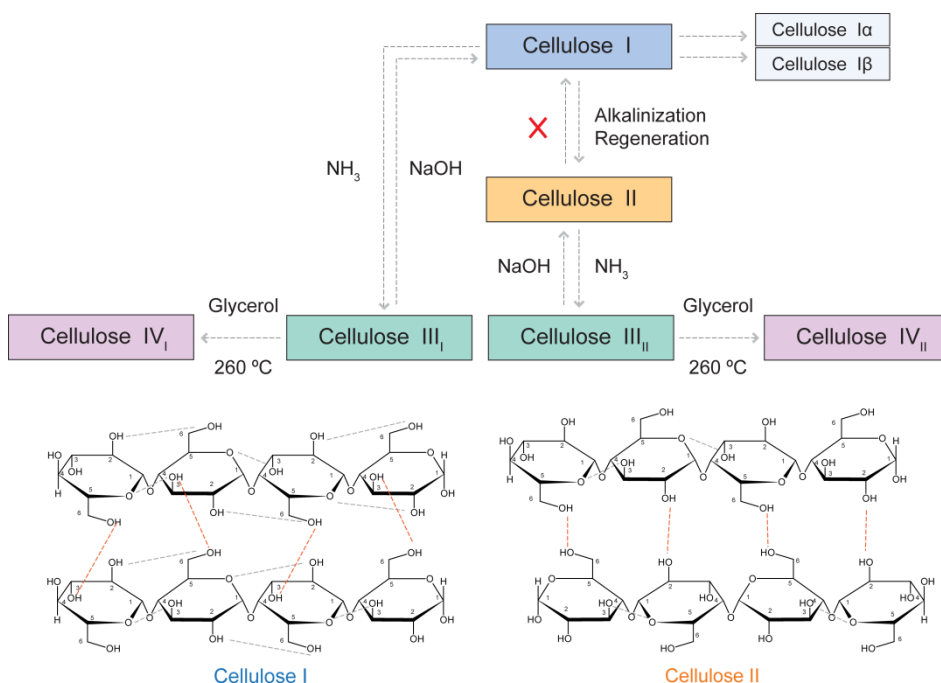


Figure 1.3. Cellulose polymorphs. We can differentiate six cellulose polymorphs depending on the inter- and intramolecular interactions of their hydrogen bonds. Cellulose I is the native and most abundant cellulose form and by chemical and physical treatments we can produce the other five.

Cellulose II is the second most abundant cellulose form; in this polymorph, the cellulose chains have an antiparallel organization. This distribution permits that the hydrogen bonds happen between the neighbor's hydroxyl groups and improved the interlayer attraction forces,

but there are less secondary hydrogen bonds [12]. These interactions made that cellulose II has added stability and produce the irreversibility to convert cellulose II into I. Also, cellulose II is more thermostable and weakly mechanically than cellulose I because of its different chain organization [13]. Cellulose II can be prepared from cellulose I by mercerization (alkaline treatment) [14] or regeneration [15]. From cellulose I and II we can produce the other polymorphs. Cellulose III is made from cellulose I or cellulose II by ammonia treatment that penetrates and degrades the cellulose crystal structure [16]. Cellulose IV is produced from cellulose III by glycerol and heat treatment at 260 °C [17]. Cellulose III can be transformed into their previous polymorphs by alkaline treatment.

In nature, cellulose is produced as an individual long chain that during the biosynthesis process is organized in a hierarchical structure to form the fibers. The polymeric chains are packed together by hydrogen bonding forming the elementary fibrils, these have a diameter of 3-5 nm and a length around 2-20 μm depending on the source [18]. These tiny fibers are aggregated by van der Waals forces and more intra and intermolecular hydrogen bonds to compose the microfibrils that have a diameter around 30 nm and a length of several micrometers, depending on the source. The orientation and packing of these microfibrils are responsible for the crystalline and amorphous fractions. The microfibrils are gathered in larger structures called macrofibrils and they are further packed into the main cellulose fibers.

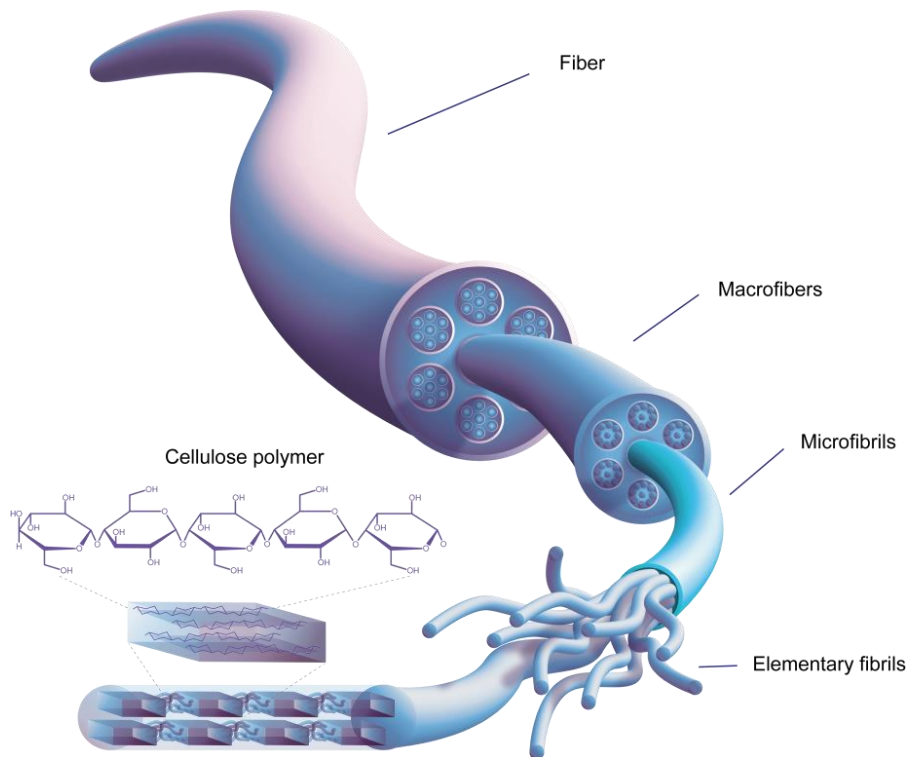


Figure 1.4. Hierarchical cellulose structure. Cellulose chains are packed together forming elementary fibrils. These tiny fibers are aggregated by hydrogen bonding and van der Waals forces into microfibrils and these are assembled in macrofibrils; the macrofibrils are the last unit that forms the main cellulose fibers.

This hierarchical structure of cellulose permits its degradation in nanoparticles, these particles are called Nanocellulose. Nanocellulose has gathered the attention of the research community and has been extensively studied since its discovering because of its extraordinary capabilities like its biocompatibility, renewability, it is sustainable, has nanometer size, large aspect ratio, and flexibility, good electrical,

thermal and mechanical features. Nanocellulose is organized in different types depending on their size, shape, crystallinity, and source: cellulose nanocrystals (CNCs) [19] have ribbon-like shape with very high crystallinity, normally have an average diameter between 2-30 nm and a length of 50 nm to 1 μm depending on the cellulose source and the isolation treatment (Table 1.1). Cellulose nanofibers (CNFs) [20] are long thin fibers with a length of several micrometers and diameters of nanometers, these fibers have both amorphous and crystalline domains. Bacterial Cellulose (BC) [21] is produced by a group of Bacteria that synthesize big thin nanofibers into the culture medium with high crystallinity, using glucose as a substrate.

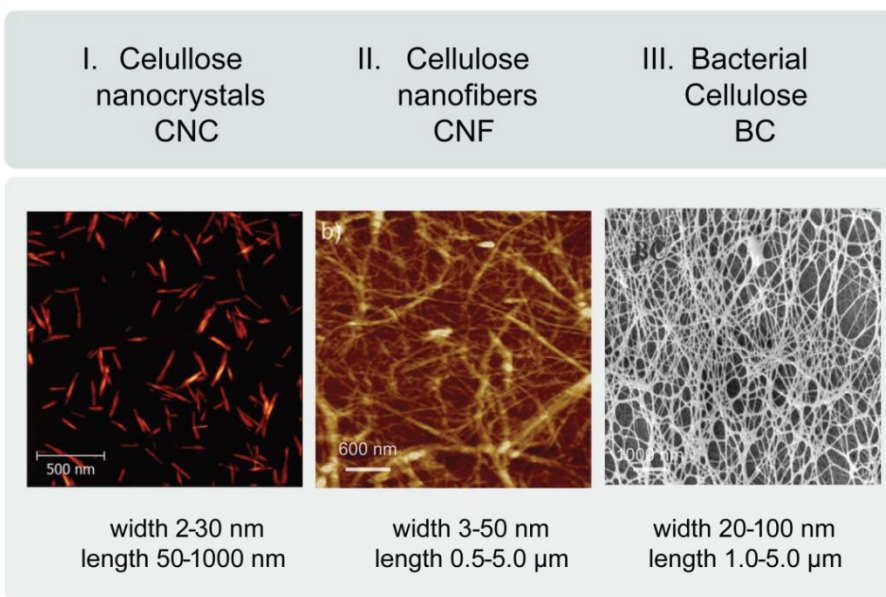


Figure 1.5. Nanocellulose types. (I) AFM image of cellulose nanocrystals (CNC) produced with sulfuric acid treatment [22], (II) AFM image of cellulose nanofibers (CNF) isolated with mechanical treatment [23], (III) SEM image of Bacterial Cellulose (BC) secreted into the culture medium and freeze-dried [24].

Due to CNCs higher crystallinity have higher mechanical properties in comparison with CNFs that have amorphous cellulose segments in its structure [25]. The CNC have also high surface area and tensile strength that can be compare to other nanomaterials used as reinforcement like kevlar or carbon nanotubes [26]. Furthermore, the morphology and degree of crystallinity on the nanocrystals affect their nanomechanical performance, a reduction on the diameter and crystallinity translate in a reduction of their strength.

Nanocellulose has several applications in different fields due to its extraordinary properties: for example, it is used as reinforcement for paper materials making strong nanopaper sheets for packaging [27, 28]. In photonics research is used to make transparent films [29], CNC can also produce iridescent films and chiral materials, and even can be modified to have other optical functionalities like UV-blocking [30] or fluorescence [31].

In biomedical research nanocellulose has a very widespread application because pure nanocellulose is relatively non-toxic and biocompatible [32], is used to made scaffolds for tissue engineering [24, 33], as a carrier for drugs [34, 35], in tissue regeneration [36], an even there are reports that nanocellulose helps fat absorption [37] in the intestine. Nanocellulose can be part of proteins composites, where nanocellulose act like reinforcement, for example to prolamin [38]. Nanocellulose films have been used for its gas barrier [39] and water absorption properties [40]. Nanocellulose can form foams and aerogels with good mechanical performances [41].

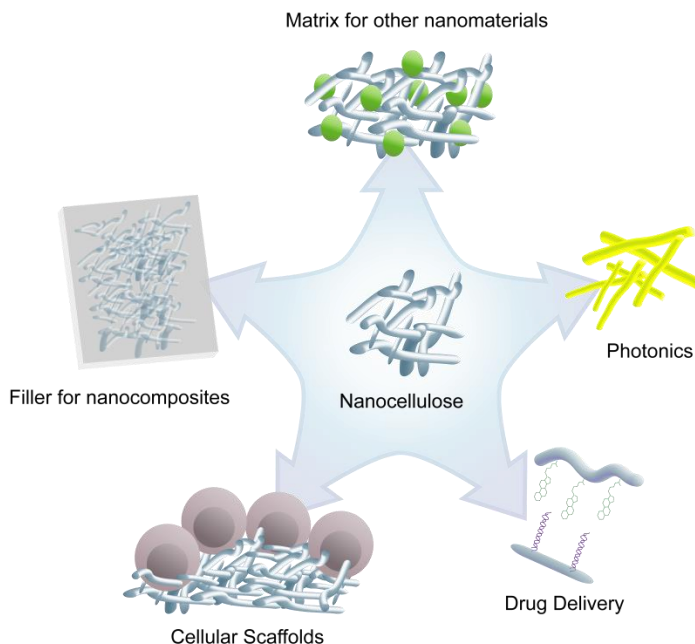


Figure 1.6. Nanocellulose application. There are several applications depending on the research field. Nanocellulose can be used as a matrix for other nanomaterials to produce nanocomposites with different properties. Nanocellulose can be used in photonic by making it fluorescent or iridescent films. In the biomedical field can be used in drug delivery systems or cellular scaffolds for tissue regeneration. One of the most common applications is as filler for nanocomposites to improve or change the mechanical and physicochemical properties of the matrix.

One of the focuses in nanocellulose application is as polymeric materials filler to manufacture a cost-effective, durable, and greener biomaterial. The physicochemical properties of nanocellulose can improve biomaterial performance. There are examples in polyvinyl alcohol (PVA) [42], polylactic acid (PLA) [43] and waterborne polyurethanes (WBPU) [44]. Due to climate change and to reduce the pollution produced by polymeric materials manufacturing, eco-friendly materials are attracting

the attention of researches, this is the case of WBPU. WBPU are capable to gather stable particles in water dispersion by addition of internal emulsifiers [45] and not using organic toxic solvent.

WBPU are block copolymers formed by two blocks or segments, the hard segment (HS) formed by urethane groups and soft segment (SS) composed by polyol [46]. These segments are thermodynamically incompatible and result in microphase separated phases or domains. The SS made the material flexible and the HS gives stiffness, but both can be ordered in amorphous or crystalline domains by hydrogen bonding (Figure 1.7)

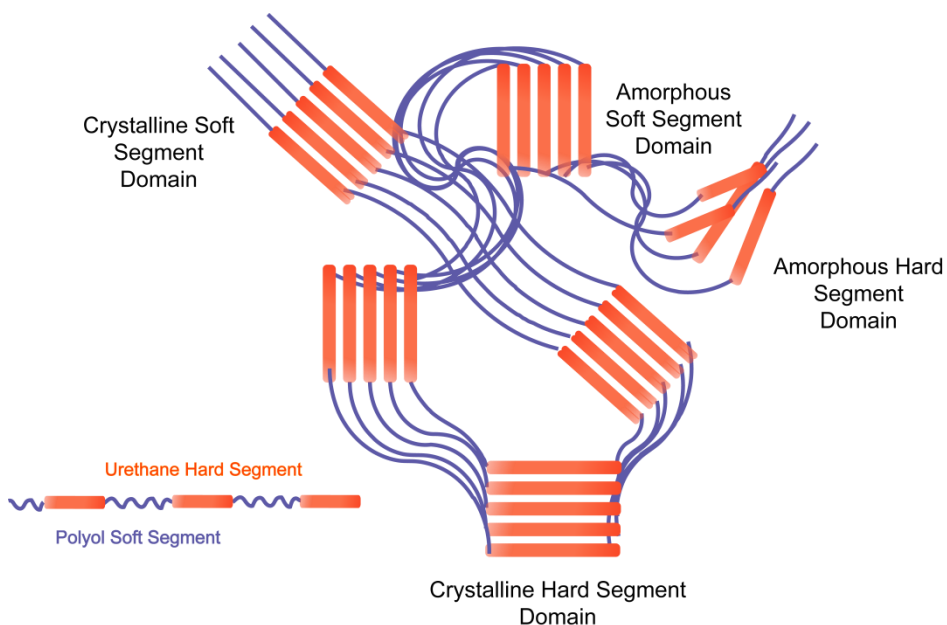


Figure 1.7. Polyurethane structure. The polyurethane is organized in two segments, the hard segment (HS) formed by the urethane group and the SS composed by the polyol. These two groups can be structured in crystalline and amorphous conformations by hydrogen bonding.

WBPU have high strength and flexibility related with the hard and soft segment. They have different applications as elastomers [47], coatings, adhesives [48, 49], polymeric dyes [50] and even in biomedical applications due to its biocompatibility [51], like tissue regeneration [52] or wound dressing [53]. Production of WBPU can be made with bio-based raw materials [54], polyols from vegetable oils can be used, like castor oil [55] or soybean oil-based macrodiol [56]. Due to these properties, this material is perfect to be filled with nanocellulose to improve its physicochemical performance [44, 57-60].

Nanocellulose has been called the new graphene due to the high interest that has generated and its possible implementation in advances materials. Graphene is a two dimensional carbon base material with a thickness of one atom, where the carbon atoms are organized in a honeycomb network by sp^2 hybridization [61, 62]. Graphene poses perfect properties for manufacturing electronic materials: large specific surface, good thermal conductivity, high charge mobility ($10000 \text{ cm}^2 \text{ s}^{-1}$) and high strength and stiffness (1 TPa of Young's Modulus) [63]. The extraordinary properties from both materials give the opportunity of manufacture new hybrids nanomaterials by their combination. A very interesting application is in flexible conductive papers that work as film transistors, energy storage and organic solar cells devices [64, 65]. This material has been built over polyethylene terephthalate (PET) [66], polycarbonate (PC) [67] or polyimide [68]. The problem of using plastic polymers are the high processing temperatures, low coefficient of thermal expansion (CTE) and they aren't renewable [69]. There are reports of films formed by graphene and cellulose [70, 71] or mixtures of

CNF and graphene oxide with conductive properties [72-75], but further investigation in the implementation of both materials are needed.

Regarding to nanocellulose isolation, different methods has been used: normally mechanical, chemical and, enzymatic treatments or a combination of two of them. The mechanical treatment consists of a high-pressure homogenization process that permits the CNF obtaining. Several mechanical processes have been used like refiners [76], cryo-crushing [77] or grinders [78]. This method needs numerous repeating steps and to reduce the energy and time consumption, chemicals like 2,2,6,6-tetramethylpiperidine-1-oxyl (TEMPO) [79] or enzymatic treatments [80] are usually used.

Table 1.1. Examples of length and diameter of CNC produced with different treatments from several sources.

Source	Length (nm)	Diameter (nm)	Treatment	Ref.
Bacterial	100 - 1000	10 - 50	Sulfuric acid	[81]
Microcrystalline cellulose	~500	10	Sulfuric acid	[82, 83]
Cotton	100 - 210	10 - 40	Sulfuric acid	[84]
Sisal	100 - 500	3 - 5	Sulfuric acid	[85]
Tunicate	100 - >1000	15 - 30	Different treatments	[86]
Wood	100 - 300	3 - 5	Sulfuric acid	[87]
Valonia	1000 - 2000	10 - 20	Sulfuric acid	[88]

The chemical treatment is the main process to manufacture CNCs and CNFs. The most common reactive used is sulfuric acid (H_2SO_4) that can swell the cellulose amorphous regions keeping the crystalline part. Depending on the time and concentration of the sulfuric acid solution, sulfate groups can be attached to the nanocrystal surface by esterification (conversion of $-OH$ groups into $-OSO_3^-$) (Figure 1.8). The usual concentration of sulfate groups can vary between 0,5 to 2% [89] and helps to stabilize the nanocrystals in water suspension but has other physicochemical consequences. The sulfuric acid treatment is optimized by using 64 wt% acid solutions at 40-50 °C for 45-60 min. The reaction is stopped by mixing the suspension with 10 fold water, centrifuged and dialyzed against water until neutral pH is reached. To achieve a good CNC dispersion sonication steps are needed during the process [90]. Other typical compounds for chemical treatment are hydrobromic acid [91], phosphoric acid [92] or TEMPO oxidation [93].

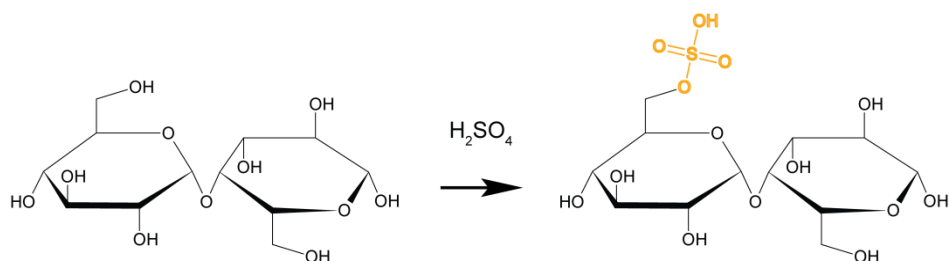


Figure 1.8. Esterification reaction in cellulose by sulfuric acid hydrolysis. Sulfuric acid treatment produces a transformation from hydroxyl groups on the nanocrystals to sulfate groups and charges negatively the surface of the particles.

The sulfuric acid treatment has some disadvantages: produces high amounts of toxic chemical residues that have a strong environmental impact. The high hydrophilicity of sulfate groups in nanocellulose made the drying process very expensive and time-consuming, and also a high volume of wastewater is produced during the washing process for neutralizing the pH after the hydrolysis [94].

We need new sustainable and efficient methods for nanocellulose isolation. The enzymatic treatment seems the best alternative because eliminates the toxic chemicals and requires less energy than mechanical production. There are some reports of nanocellulose isolation using enzymes in the literature in recent years. The first investigations used the combination of enzymatic and mechanical treatments to improve the cellulose microfibrillation [95]. Other reports from Filson et al. [96] explored the nanocellulose preparation using fungal endoglucanases and microwave heating treatments to Softwood Kraft pulp. These studies were followed by others where commercial endoglucanase were used in combinational protocols for nanocellulose production from different lignocellulose substrates like Bleached eucalyptus fibers [97, 98], old corrugated container fibers [99], Bleached Softwood Kraft pulp [100], Bleached Hardwood Kraft pulp [101], cotton [102], citrus waste [103], bacterial nanocellulose [104], microcrystalline cellulose [105] or sugarcane [106]. In 2017, Yarbrough et al. reported the use of the total exoproteome of the fungi *Trichoderma reesei* and the hyperthermophile bacteria *Caldicellulosiruptor bescii* on Bleached Kraft pulp achieving nanocellulose isolation.

To optimize the enzymatic treatment, we need to develop new enzymes with higher catalytic and promiscuous activity, and they need to work in different conditions. The more common protein engineering techniques for protein improvement are Rational Design and Directed Evolution. Rational Design [107, 108] consist on the mutagenesis of specific amino acids in the protein sequences. To achieve success with this technique it will require proteins with well-known structure and a studied mechanism that usually is not available. With Directed Evolution [109, 110] techniques changes can be produced in the amino acid sequences in an aleatory way. In this case, it's needed to produce and test a large library of mutants to obtain a protein with the features of interest, making this process very time and cost consuming.

A new approach in protein engineering is ancestral sequence reconstruction (ASR), normally used for evolution studies [111]. This technique permits us to bring back to life proteins from millions of years ago that were adapted to work in a totally different environment and had different properties in comparison with the nowadays enzymes. There are several reports in the bibliography that showed how the ancestral enzymes have more specific activities, are more promiscuous [112] and thermostable [113, 114] than extant enzymes. This extraordinary characteristic makes these ancestral enzymes suitable for biotechnology applications [115].

This technique consists of several bioinformatical and biomolecular steps. First, DNA or amino acids sequences from proteins of extant organisms are gathered from online databases, these sequences are then

analyzed by bioinformatics tools to calculate a phylogenetic tree that represents the evolutionary relationship between the proteins selected. By further informatics analysis, the sequence from the ancestors of each node of the tree can be inferred and the sequences are synthesized. By biomolecular tools we can produce these proteins in the laboratory. In this way, we can obtain several ancestral proteins, depending on the size of the tree, with different characteristic depending on the million years that they have and the node that we selected. This made this technique more efficient than the alternatives that need to produce a larger amount of proteins to achieve a desired one.

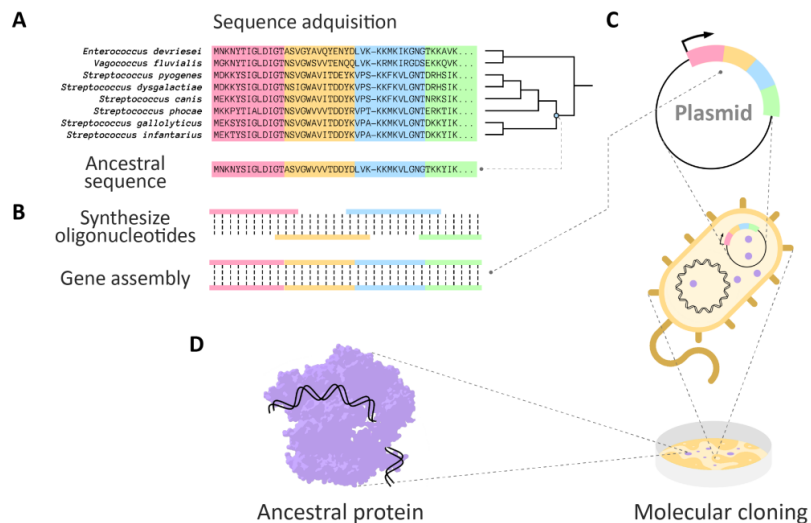


Figure 1.9. Ancestral sequence reconstruction. (A) Amino acids sequences from extant organisms are aligned and a phylogenetic tree is inferred with bioinformatical tool, (B) Sequences from the ancestral proteins are calculated from the nodes of the tree. (C) Expression plasmid with the gen from the ancestral protein and the bacterial host for protein expression. (D) Ancestral proteins expressed from the bacterial host.

Cellulases are enzymes produced by several organisms, the most common are bacteria and fungi, that degrade the cellulose polymer by breaking the β -1,4-glycosidic bonds. The total degradation of cellulose into glucose monomers needs three cellulases (Figure 1.10): Endoglucanase (EG) that degrades the cellulose chains in random locations to produce oligomers with reducing ends; preferably attack the amorphous regions of the fibers. Exoglucanase (CBH) that breaks down the crystalline cellulose and degrade the previous reducing oligomers into cellobiose units, working synergistically with EGs [116] and β -glucosidase (BG) that hydrolyzes cellobiose into glucose monomers [117].

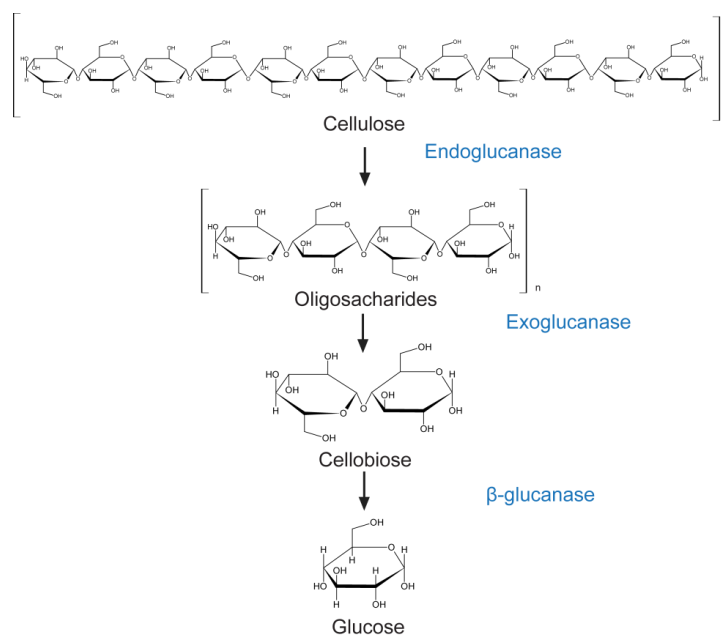


Figure 1.10. Enzymatic cellulose degradation by cellulases. Endoglucanase (EG) breaks down the cellulose polymer into oligosaccharides breaking the β -1,4-glycosidic bonds randomly. Exoglucanase (CBH) hydrolyzes oligosaccharides with reducing ends produced by EG into cellobiose units and β -glucosidase (BG) breaks the cellobiose unit into the glucose monomers.

Cellulases have different structures: they can have a single catalytic domain or be bound by a flexible linker to a Carbohydrate-Binding Module (CBM). CBMs help the attachment of the catalytic domain into the cellulose surface, improving its catalytic activity [118, 119]. The CBM also help the activity on insoluble and recalcitrant substrates as crystalline cellulose [120]. In nature, exists cellulases structured in a complex system called cellulosome that is produced by some anaerobic bacteria [121]. The structure is composed of non-catalytic proteins known as dockerins and cohesins that formed a protein scaffold [122], attached to this structure are several enzymes with different catalytic activities. This assemble has higher activity in an insoluble substrate than free enzymes [123]. There are several reports of designer chimeric cellulosome in the lab to improve the catalytic activity [124], but this big structure is hard to produce.

Cellulases are not the only enzymes that can attack the cellulose polymer; recently the discovery of the lytic polysaccharides monooxygenases (LPMO) has attracted the attention of the lignocellulosic research community. LPMOs are produced by fungi and bacteria [125], even is found in some virus [126]. LPMOs are copper-enzymes that produce oxidative cleave on the glycosidic bonds, first were studied their activity in crystalline chitin [127] and cellulose [128], but they showed activity on other polymers as hemicellulose [129] or starch [130]. LPMO oxidation is proposed to produce chain cleavage, the chain break is made on C₁ or C₄ carbon of glucose (Figure 1.11), even in C₆ in some cases [131]. C₁ oxidation produces soluble oligosaccharides with an aldonic acid in the reducing end and C₄ oxidation generates a

keltoaldose in the non-reducing end [128, 132]. There are LPMO that oxidate both C₁ and C₄ like the LPMO from *Streptomyces coelicolor* [133, 134] or oxidate selectively one of the C like the LPMO from *Myceliophthora thermophila* [135]. Since their discovery, several reports of using LPMO in combination with cellulases in biomass conversion has been published [136-138], the LPMO boost cellulases activity by making new cleavage in the chains helping the cellulases to attack the crystalline cellulose [139].

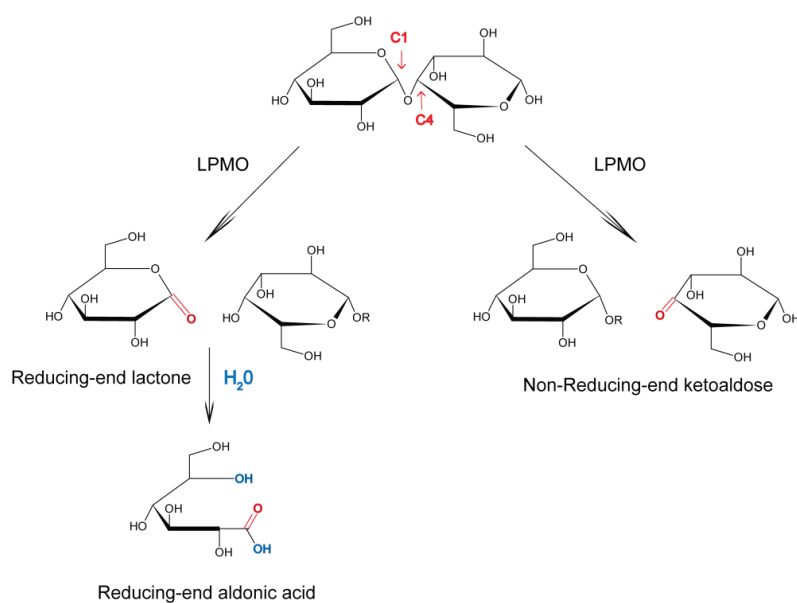


Figure 1.11. LPMO catalytic activity. LPMO can break the cellulose polymer by oxidation of C₁ or C₄ carbon in general. C₁ oxidation leads to soluble oligosaccharides with an aldonic acid in the reducing end and C₄ oxidation produces a ketoaldose in the non-reducing end.

Cellulose is not alone in the lignocellulosic biomass, there are two more main components: hemicellulose, a heteropolymer composed by different sugars [140], and lignin, aromatic polymers formed by phenylpropanoid

precursors [141]. Cellulose composes around the 45% of the biomass dry weight, hemicellulose is the second most abundant with 25-30% and lignin is present around 20-10%. The three components are in different concentration depending on the source and the plant age [142]. For the proper cellulose isolation it is necessary to liberate it from the lignocellulosic matrix.

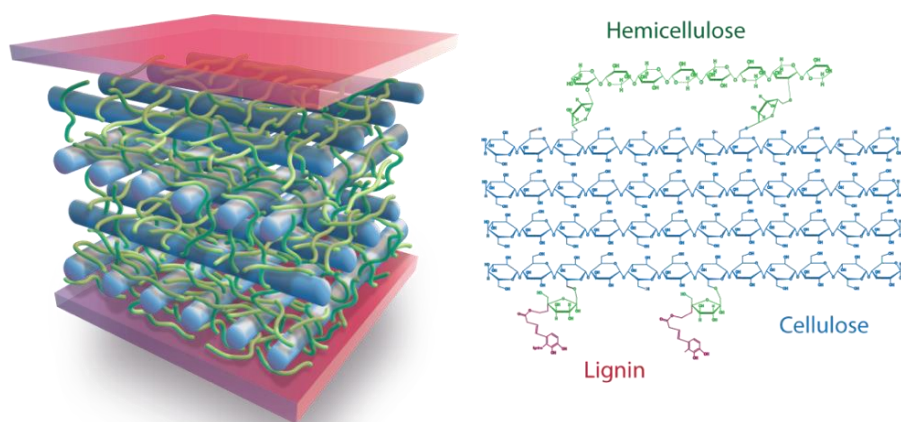


Figure 1.12. Lignocellulosic biomass. Cellulose fibers are located between a matrix of hemicellulose and lignin. Hemicellulose is composed by monosaccharides of 5 or 6 sugars binding together by β -glycosidic bond and lignin is form by phenylpropanoid precursors. Hemicellulose is bonded to cellulose and lignin by hydrogen and covalent bonding producing a very recalcitrant and stiff structure. This structure needs to be degraded in order to liberate cellulose fibers for further cellulose conversion into nanocellulose or sugars.

Hemicellulose structure consists of different carbohydrate polymers; the main polymer is xylan or glucomannan but has other sugars like xyloses,

arabinoses, glucose, galactose, mannose, and sugar acids. Hemicellulose is easier to degrade than cellulose due to the lower molecular weight and the short lateral branches that form the polymer [143]. Hemicellulose is linked to cellulose by hydrogen bonding and covalently to lignin, giving stiffness to the lignocellulose matrix [144, 145]. The hemicellulose can be extracted from biomass with sulfuric acid [146], alkaline pretreatment [147], steam explosion [148], mechanical treatments [149] but also can be removed by enzymatic hydrolysis. The most used enzyme is the Endo-1,4- β -xylanase that degrades the xylan polymer into oligosaccharides by breaking the β -glycosidic bonds between the monomers. Xylanase is produced by bacteria or fungi [150] and has been used in biomass degradation in process like paper pulp bleaching [151, 152].

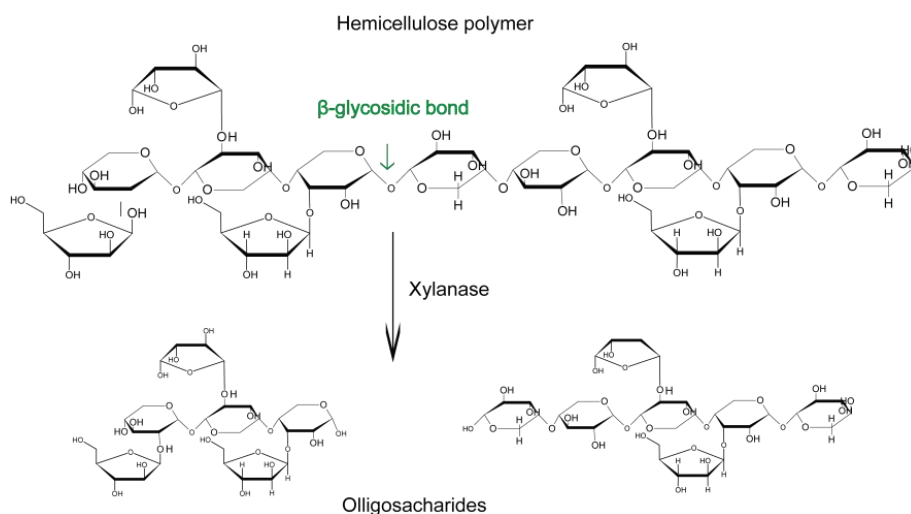


Figure 1.13. Xylanase catalytic reaction. Xylanase is able to break down the β -glycosidic bond between the xylan polymers and produces small oligosaccharides as product.

Lignin is a physical barrier that protects cellulose fibers due to its structural complexity, high molecular weight, and insolubility. The linkage between lignin, cellulose, and hemicellulose are believed that inhibit the enzyme activity [153]. Chemical and physicochemical treatment can be used to disrupt lignin structure [154, 155]. There are two main families of enzymes that can depolymerize lignin too: peroxidases and laccase, produced mainly by the lignolytic white-rot fungi [156] and higher plant, but also found in bacteria [157].

The principal objective of this thesis is to prove that ancestral reconstructed enzymes can have a potential industrial application in nanocellulose production as an alternative to the actual methods. At first, we focused in the nanocellulose isolation by ancestral endoglucanase (LFCA or ANC EG) that could improve the process where the extant enzyme fails due to its capability of degrading several substrates and its higher activity in different conditions than extant endoglucanases (Figure 1.14) from *Bacillus subtilis* or the extremophyllic *Thermotoga maritima* [158]. During the thesis, we also characterized with different physicochemical analysis the nanocellulose obtained by enzymatic treatment and found that they had different properties in comparison with commercial nanocellulose isolated with sulfuric acid treatment.

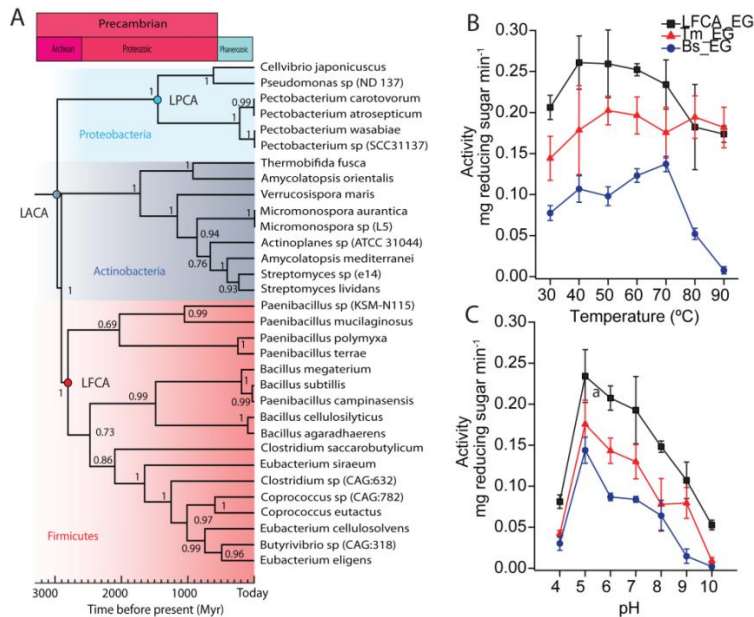


Figure 1.14. Ancestral endoglucanase reconstruction. (A) In previous work in the Nanobiomechanics group (CIC nanoGune), the ancestral reconstruction of bacterial endoglucanase was performed and the node of the last firmicute common ancestor (LFCA) of the tree was characterized. We observed that the ancestral EG has higher activity in a broad range of temperature (B) and pH (C) than extant EG from *B. subtilis* or the *T. maritima*.

Once we optimized the process, the second objective that we had was to produce nanocellulose from lignocellulosic biomass. For that purpose we used an ancestral enzymatic cocktail with the addition of xylanase and LPMO in the treatment, these enzymes were reconstructed and characterized in a parallel work in the Nanobiomechanics group (CIC nanoGune). We found during these studies that we can modify nanocellulose by oxidation with an ancestral LPMO in a similar way that chemicals do.

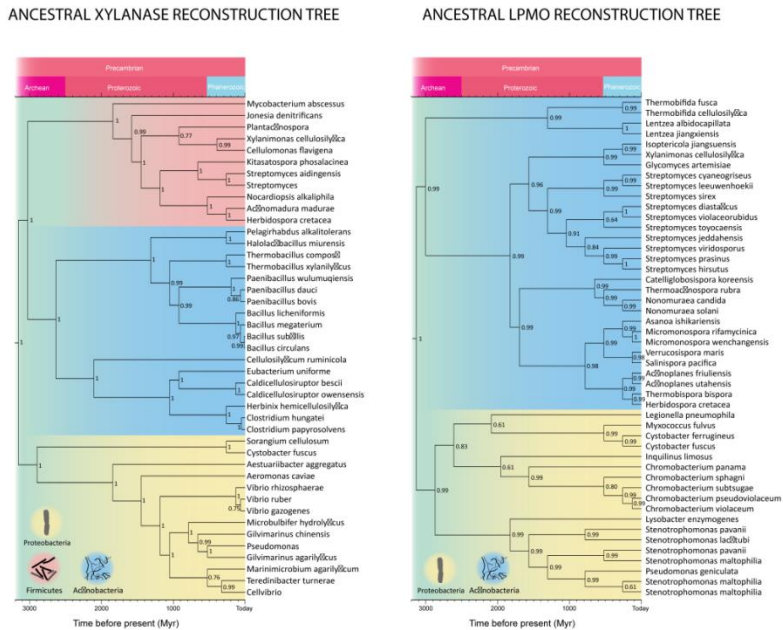


Figure 1.15. Ancestral xylanase and LPMO reconstruction. In a parallel thesis in the Nanobiomechanics group (CIC nanoGUNE); we reconstructed these two enzymes for an ancestral enzymatic cocktail production to achieve nanocellulose isolation from lignocellulosic substrates.

We studied two applications for nanocellulose isolated by enzymatic treatment (EnCNC), and also compared its performances respect to AcCNC. We found that our enzymatic nanocellulose used as WBPU filler have better mechanical and thermal performance than commercial nanocellulose produced by sulfuric acid. Also, we found that our nanocellulose can form films with nanopaper-like structure. This particular characteristic permitted us to made nanopapers with conductive properties mixing our nanocellulose with graphene, these nanopapers showed good thermal, mechanical and conductive properties. For conductive nanopapers manufacturing we even propose a new

strategy by using nanocellulose films as a substrate for Chemical Vapour Deposition of graphene, in order to substitute the plastic or metal substrates.

Objectives

The main objectives on this thesis were the optimization of a new method for nanocellulose isolation using ancestral enzymes from different sources, its characterization and applications. This work was carried out in three parts:

1. This part of the thesis involved the nanocellulose isolation by ancestral endoglucanase:
 - Development and optimization of a new method for nanocellulose isolation by ancestral endoglucanase from filter paper.
 - The study of the size and morphology of the nanocellulose produced at different hydrolysis time.
 - The physicochemical and morphological characterization of this enzymatically produced nanocellulose and its comparison with a commercial sample of cellulose nanocrystals isolated by sulfuric acid hydrolysis.
2. The second part was focused on nanocellulose isolation from two lignocellulosic substrates with the optimized method.
 - The addition of new ancestral enzymes as xylanase and lytic polysaccharide monooxygenase (LPMO) to help the ancestral endoglucanase activity.
 - The study of the effect of the complex substrates on the nanocellulose yield.
 - The physicochemical and morphological characterization of this new nanocellulose.

3. In the final part we studied two applications for the enzymatic nanocellulose and its comparison with the commercial sample in the same conditions.
 - The effect of nanocellulose as reinforcement in polymeric nanocomposites.
 - Preparation and final properties of nanocomposites based on polyurethanes and different content of nanocellulose isolated in this thesis by ancestral enzymes and commercial nanocellulose isolated by sulfuric acid treatment.
 - Produce conductive nanopapers by different strategies for graphene addition to enzymatic nanocellulose films.

This multidisciplinary work has been possible thanks to the collaboration of two research groups. The ancestral sequence reconstruction of the enzymes used in this thesis and the nanocellulose isolation was carried out in the Nanobiomechanics group from CIC nanoGune, specialist in ancestral protein reconstruction and its characterization. The characterization of the nanocellulose produced with the different enzymatic treatments and the materials fabricated in this thesis were carried out in the Materials + Technologies Group (GMT) of the Chemical and Environmental Engineering Department of the Basque Country University (UPV/EHU). This research group has the experience in nanocellulose characterization and its implementation in several applications. This work was funded by the Elkartek project from the Basque Country Government.

Bibliography

1. Schweiger-Hufnagel, U., et al., *Identification of the extracellular polysaccharide produced by the snow mold fungus microdochium nivale*. *Biotechnol. Lett.*, 2000. 22(3): p. 183-187.
2. Iguchi, M., Yamanaka, S., and Budhiono, A., *Bacterial cellulose—a masterpiece of nature's arts*. *J. Mater. Sci.*, 2000. 35(2): p. 261-270.
3. Mhryanyan, A., *Cellulose from cladophorales green algae: From environmental problem to high-tech composite materials*. *J. Appl. Polym. Sci.*, 2011. 119(4): p. 2449-2460.
4. Zhao, Y. and Li, J., *Excellent chemical and material cellulose from tunicates: Diversity in cellulose production yield and chemical and morphological structures from different tunicate species*. *Cellulose*, 2014. 21(5): p. 3427-3441.
5. Klemm, D., et al., *Cellulose: Fascinating biopolymer and sustainable raw material*. *Angew. Chem.*, 2005. 44(22): p. 3358-3393.
6. Pinkert, A., et al., *Ionic liquids and their interaction with cellulose*. *Chem. Rev.*, 2009. 109(12): p. 6712-6728.
7. Mazeau, K. and Heux, L., *Molecular dynamics simulations of bulk native crystalline and amorphous structures of cellulose*. *J. Phys. Chem. B*, 2003. 107(10): p. 2394-2403.
8. Ciolacu, D., Ciolacu, F., and Popa, V.I., *Amorphous cellulose—structure and characterization*. *Cell. Chem. Technol.*, 2011. 45(1): p. 13.
9. Atalla, R.H. and Vanderhart, D.L., *Native cellulose: A composite of two distinct crystalline forms*. *Science*, 1984. 223(4633): p. 283-285.
10. Nishiyama, Y., et al., *Crystal structure and hydrogen bonding system in cellulose Ia from synchrotron x-ray and neutron fiber diffraction*. *J. Am. Chem. Soc.*, 2003. 125(47): p. 14300-14306.
11. Nishiyama, Y., Langan, P., and Chanzy, H., *Crystal structure and hydrogen-bonding system in cellulose Ib from synchrotron x-ray and neutron fiber diffraction*. *J. Am. Chem. Soc.*, 2002. 124(31): p. 9074-9082.

12. Langan, P., Nishiyama, Y., and Chanzy, H., *A revised structure and hydrogen-bonding system in cellulose ii from a neutron fiber diffraction analysis*. *J. Am. Chem. Soc.*, 1999. 121(43): p. 9940-9946.
13. Yue, Y., Han, G., and Wu, Q., *Transitional properties of cotton fibers from cellulose i to cellulose ii structure*. *BioResources*, 2013. 8(4): p. 6460-6471.
14. Jin, E., et al., *On the polymorphic and morphological changes of cellulose nanocrystals (cnc-i) upon mercerization and conversion to cnc-ii*. *Carbohydr. Polym.*, 2016. 143: p. 327-335.
15. Zhang, Y.-H.P., et al., *A transition from cellulose swelling to cellulose dissolution by o-phosphoric acid: Evidence from enzymatic hydrolysis and supramolecular structure*. *Biomacromolecules*, 2006. 7(2): p. 644-648.
16. Wada, M., et al., *Cellulose iii crystal structure and hydrogen bonding by synchrotron x-ray and neutron fiber diffraction*. *Macromolecules*, 2004. 37(23): p. 8548-8555.
17. Wada, M., Heux, L., and Sugiyama, J.J.B., *Polymorphism of cellulose i family: Reinvestigation of cellulose ivi*. *Biomacromolecules*, 2004. 5(4): p. 1385-1391.
18. Frey-Wyssling, A., *The fine structure of cellulose microfibrils*. *Science*, 1954. 119(3081): p. 80-82.
19. Habibi, Y., Lucia, L.A., and Rojas, O.J.J.C.r., *Cellulose nanocrystals: Chemistry, self-assembly, and applications*. *Chem. Rev.*, 2010. 110(6): p. 3479-3500.
20. Saito, T., et al., *Cellulose nanofibers prepared by tempo-mediated oxidation of native cellulose*. *Biomacromolecules*, 2007. 8(8): p. 2485-2491.
21. Rehm, B.H., *Bacterial polymers: Biosynthesis, modifications and applications*. *Nat. Rev. Microbiol.*, 2010. 8(8): p. 578.
22. Brinkmann, A., et al., *Correlating cellulose nanocrystal particle size and surface area*. *Langmuir*, 2016. 32(24): p. 6105-6114.
23. Berglund, L., et al., *Promoted hydrogel formation of lignin-containing arabinoxylan aerogel using cellulose nanofibers as a functional biomaterial*. *RSC Adv.*, 2018. 8(67): p. 38219-38228.
24. Svensson, A., et al., *Bacterial cellulose as a potential scaffold for tissue engineering of cartilage*. *Biomaterials*, 2005. 26(4): p. 419-431.

25. Yildirim, N. and Shaler, S., *A study on thermal and nanomechanical performance of cellulose nanomaterials (cns)*. *Materials*, 2017. 10(7): p. 718.
26. Moon, R.J., et al., *Cellulose nanomaterials review: Structure, properties and nanocomposites*. *Chem. Soc. Rev.*, 2011. 40(7): p. 3941-3994.
27. Henriksson, M., et al., *Cellulose nanopaper structures of high toughness*. *Biomacromolecules*, 2008. 9(6): p. 1579-1585.
28. Sehaqui, H., et al., *Strong and tough cellulose nanopaper with high specific surface area and porosity*. *Biomacromolecules*, 2011. 12(10): p. 3638-3644.
29. Xue, J., et al., *Let it shine: A transparent and photoluminescent foldable nanocellulose/quantum dot paper*. *ACS Appl. Mater. Interfaces*, 2015. 7(19): p. 10076-10079.
30. Feng, X., et al., *Use of carbon dots to enhance uv-blocking of transparent nanocellulose films*. *Carbohydr. Polym.*, 2017. 161: p. 253-260.
31. Díez, I., et al., *Functionalization of nanofibrillated cellulose with silver nanoclusters: Fluorescence and antibacterial activity*. *Macromol. Biosci.*, 2011. 11(9): p. 1185-1191.
32. Jia, B., et al., *Effect of microcrystal cellulose and cellulose whisker on biocompatibility of cellulose-based electrospun scaffolds*. *Cellulose*, 2013. 20(4): p. 1911-1923.
33. He, X., et al., *Uniaxially aligned electrospun all-cellulose nanocomposite nanofibers reinforced with cellulose nanocrystals: Scaffold for tissue engineering*. *Biomacromolecules*, 2014. 15(2): p. 618-627.
34. Dash, R. and Ragauskas, A.J., *Synthesis of a novel cellulose nanowhisker-based drug delivery system*. *RSC Adv.*, 2012. 2(8): p. 3403-3409.
35. Silva, N.H., et al., *Bacterial cellulose membranes as transdermal delivery systems for diclofenac: In vitro dissolution and permeation studies*. *Carbohydr. Polym.*, 2014. 106: p. 264-269.
36. Ávila, H.M., et al., *Biocompatibility evaluation of densified bacterial nanocellulose hydrogel as an implant material for auricular cartilage regeneration*. *Appl. Microbiol. Biotechnol.*, 2014. 98(17): p. 7423-7435.
37. DeLoid, G.M., et al., *Reducing intestinal digestion and absorption of fat using a nature-derived biopolymer:*

- Interference of triglyceride hydrolysis by nanocellulose.* ACS nano, 2018.
38. Wang, Y. and Chen, L., *Cellulose nanowhiskers and fiber alignment greatly improve mechanical properties of electrospun prolamin protein fibers.* ACS Appl. Mater. Interfaces, 2014. 6(3): p. 1709-1718.
 39. Nair, S.S., et al., *High performance green barriers based on nanocellulose.* Sustain. Chem. Process., 2014. 2(1): p. 23.
 40. Belbekhouche, S., et al., *Water sorption behavior and gas barrier properties of cellulose whiskers and microfibrils films.* Carbohydr. Polym., 2011. 83(4): p. 1740-1748.
 41. Dash, R., Li, Y., and Ragauskas, A.J., *Cellulose nanowhisker foams by freeze casting.* Carbohydr. Polym., 2012. 88(2): p. 789-792.
 42. Asad, M., et al., *Preparation and characterization of nanocomposite films from oil palm pulp nanocellulose/poly (vinyl alcohol) by casting method.* Carbohydr. Polym., 2018. 191: p. 103-111.
 43. Fortunati, E., et al., *Effects of modified cellulose nanocrystals on the barrier and migration properties of pla nanobiocomposites.* Carbohydr. Polym., 2012. 90(2): p. 948-956.
 44. Gao, Z., et al., *Biocompatible elastomer of waterborne polyurethane based on castor oil and polyethylene glycol with cellulose nanocrystals.* Carbohydr. Polym., 2012. 87(3): p. 2068-2075.
 45. Nelson, A.M. and Long, T.E., *Synthesis, properties, and applications of ion-containing polyurethane segmented copolymers.* Macromol. Chem. Phys., 2014. 215(22): p. 2161-2174.
 46. Jaudouin, O., et al., *Ionomer-based polyurethanes: A comparative study of properties and applications.* Polym. Int., 2012. 61(4): p. 495-510.
 47. Jiang, X., et al., *Synthesis and degradation of nontoxic biodegradable waterborne polyurethanes elastomer with poly (ϵ -caprolactone) and poly (ethylene glycol) as soft segment.* Eur. Polym. J., 2007. 43(5): p. 1838-1846.
 48. Hu, W., Patil, N.V., and Hsieh, A.J., *Glass transition of soft segments in phase-mixed poly (urethane urea) elastomers by time-domain 1h and 13c solid-state nmr.* Polymer, 2016. 100: p. 149-157.

49. Perez-Liminana, M.A., et al., *Characterization of waterborne polyurethane adhesives containing different amounts of ionic groups*. *Int. J. Adhes. Adhes.*, 2005. 25(6): p. 507-517.
50. Mao, H., et al., *Synthesis of blocked waterborne polyurethane polymeric dyes with tailored molecular weight: Thermal, rheological and printing properties*. *RSC Adv.*, 2016. 6(62): p. 56831-56838.
51. Sartori, S., et al., *Biomimetic polyurethanes in nano and regenerative medicine*. *J. Mater. Chem. B*, 2014. 2(32): p. 5128-5144.
52. Hung, K.-C., et al., *Water-based polyurethane 3d printed scaffolds with controlled release function for customized cartilage tissue engineering*. *Biomaterials*, 2016. 83: p. 156-168.
53. Yoo, H.J. and Kim, H.D., *Characteristics of waterborne polyurethane/poly (n-vinylpyrrolidone) composite films for wound-healing dressings*. *J. Appl. Polym. Sci.*, 2008. 107(1): p. 331-338.
54. Remya, V., et al., *Biobased materials for polyurethane dispersions*. *Chem. Int.*, 2016. 2(3): p. 158-167.
55. Madbouly, S.A., Xia, Y., and Kessler, M.R., *Rheological behavior of environmentally friendly castor oil-based waterborne polyurethane dispersions*. *Macromolecules*, 2013. 46(11): p. 4606-4616.
56. Lu, Y. and Larock, R.C., *Soybean-oil-based waterborne polyurethane dispersions: Effects of polyol functionality and hard segment content on properties*. *Biomacromolecules*, 2008. 9(11): p. 3332-3340.
57. Saralegi, A., et al., *The role of cellulose nanocrystals in the improvement of the shape-memory properties of castor oil-based segmented thermoplastic polyurethanes*. *Compos. Sci. Technol.*, 2014. 92: p. 27-33.
58. Mondragon, G., et al., *Nanocomposites of waterborne polyurethane reinforced with cellulose nanocrystals from sisal fibres*. *J. Polym. Environ.*, 2018. 26(5): p. 1869-1880.
59. Santamaria-Echart, A., et al., *Two different incorporation routes of cellulose nanocrystals in waterborne polyurethane nanocomposites*. *Eur. Polym. J.*, 2016. 76: p. 99-109.
60. Santamaria-Echart, A., et al., *Cellulose nanocrystals reinforced environmentally-friendly waterborne polyurethane nanocomposites*. *Carbohydr. Polym.*, 2016. 151: p. 1203-1209.

61. Geim, A.K., *Graphene: Status and prospects*. Science, 2009. 324(5934): p. 1530-1534.
62. Stankovich, S., et al., *Graphene-based composite materials*. Nature, 2006. 442(7100): p. 282.
63. Wei, Z., et al., *Nanoscale tunable reduction of graphene oxide for graphene electronics*. Science, 2010. 328(5984): p. 1373-1376.
64. Gomez De Arco, L., et al., *Continuous, highly flexible, and transparent graphene films by chemical vapor deposition for organic photovoltaics*. ACS nano, 2010. 4(5): p. 2865-2873.
65. El-Kady, M.F., et al., *Laser scribing of high-performance and flexible graphene-based electrochemical capacitors*. Science, 2012. 335(6074): p. 1326-1330.
66. Moon, I.K., et al., *Reduced graphene oxide by chemical graphitization*. Nat. Commun., 2010. 1: p. 73.
67. Kim, H. and Macosko, C.W., *Processing-property relationships of polycarbonate/graphene composites*. Polymer, 2009. 50(15): p. 3797-3809.
68. Yoonessi, M., et al., *Graphene polyimide nanocomposites; thermal, mechanical, and high-temperature shape memory effects*. ACS nano, 2012. 6(9): p. 7644-7655.
69. Mecking, S.J.A.C.I.E., *Nature or petrochemistry?—biologically degradable materials*. Angew. Chem., 2004. 43(9): p. 1078-1085.
70. Dikin, D.A., et al., *Preparation and characterization of graphene oxide paper*. Nature, 2007. 448(7152): p. 457.
71. Chen, H., et al., *Mechanically strong, electrically conductive, and biocompatible graphene paper*. Adv. Mater., 2008. 20(18): p. 3557-3561.
72. Kang, Y.-R., et al., *Fabrication of electric papers of graphene nanosheet shelled cellulose fibres by dispersion and infiltration as flexible electrodes for energy storage*. Nanoscale, 2012. 4(10): p. 3248-3253.
73. Dang, L.N. and Seppälä, J.J.C., *Electrically conductive nanocellulose/graphene composites exhibiting improved mechanical properties in high-moisture condition*. Cellulose, 2015. 22(3): p. 1799-1812.
74. Luong, N.D., et al., *Graphene/cellulose nanocomposite paper with high electrical and mechanical performances*. J. Mater. Chem., 2011. 21(36): p. 13991-13998.

75. Hou, M., et al., *Enhanced electrical conductivity of cellulose nanofiber/graphene composite paper with a sandwich structure*. ACS Sustain. Chem. Eng., 2018. 6(3): p. 2983-2990.
76. Dufresne, A. and Vignon, M.R., *Improvement of starch film performances using cellulose microfibrils*. Macromolecules, 1998. 31(8): p. 2693-2696.
77. Alemdar, A. and Sain, M., *Isolation and characterization of nanofibers from agricultural residues—wheat straw and soy hulls*. Bioresour. Technol., 2008. 99(6): p. 1664-1671.
78. Iwamoto, S., Nakagaito, A., and Yano, H., *Nano-fibrillation of pulp fibers for the processing of transparent nanocomposites*. Appl. Phys. A, 2007. 89(2): p. 461-466.
79. Isogai, T., Saito, T., and Isogai, A., *Wood cellulose nanofibrils prepared by tempo electro-mediated oxidation*. Cellulose, 2011. 18(2): p. 421-431.
80. Henriksson, M., et al., *An environmentally friendly method for enzyme-assisted preparation of microfibrillated cellulose (mfc) nanofibers*. Eur. Polym. J., 2007. 43(8): p. 3434-3441.
81. Hirai, A., et al., *Phase separation behavior in aqueous suspensions of bacterial cellulose nanocrystals prepared by sulfuric acid treatment*. Langmuir, 2008. 25(1): p. 497-502.
82. Haafiz, M.M., et al., *Isolation and characterization of cellulose nanowhiskers from oil palm biomass microcrystalline cellulose*. Carbohydr. Polym., 2014. 103: p. 119-125.
83. Bondeson, D., Mathew, A., and Oksman, K., *Optimization of the isolation of nanocrystals from microcrystalline cellulose by acid hydrolysis*. Cellulose, 2006. 13(2): p. 171.
84. Morais, J.P.S., et al., *Extraction and characterization of nanocellulose structures from raw cotton linter*. Carbohydr. Polym., 2013. 91(1): p. 229-235.
85. Mariano, M., Cercená, R., and Soldi, V., *Thermal characterization of cellulose nanocrystals isolated from sisal fibers using acid hydrolysis*. Ind. Crops, Prod., 2016. 94: p. 454-462.
86. Zhao, Y., et al., *Tunicate cellulose nanocrystals: Preparation, neat films and nanocomposite films with glucomannans*. Carbohydr. Polym., 2015. 117: p. 286-296.
87. Chen, L., et al., *Tailoring the yield and characteristics of wood cellulose nanocrystals (cnc) using concentrated acid hydrolysis*. Cellulose, 2015. 22(3): p. 1753-1762.

88. Imai, T., et al., *Unidirectional processive action of cellobiohydrolase cel7a on valonia cellulose microcrystals*. FEBS Lett., 1998. 432(3): p. 113-116.
89. Håkansson, H. and Ahlgren, P., *Acid hydrolysis of some industrial pulps: Effect of hydrolysis conditions and raw material*. Cellulose, 2005. 12(2): p. 177-183.
90. Zhong, L., et al., *Colloidal stability of negatively charged cellulose nanocrystalline in aqueous systems*. Carbohydr. Polym., 2012. 90(1): p. 644-649.
91. Sadeghifar, H., et al., *Production of cellulose nanocrystals using hydrobromic acid and click reactions on their surface*. J. Mater. Sci., 2011. 46(22): p. 7344-7355.
92. Camarero Espinosa, S., et al., *Isolation of thermally stable cellulose nanocrystals by phosphoric acid hydrolysis*. Biomacromolecules, 2013. 14(4): p. 1223-1230.
93. Zhou, Y., et al., *Acid-free preparation of cellulose nanocrystals by tempo oxidation and subsequent cavitation*. Biomacromolecules, 2018. 19(2): p. 633-639.
94. Johar, N., et al., *Extraction, preparation and characterization of cellulose fibres and nanocrystals from rice husk*. Ind. Crops Prod., 2012. 37(1): p. 93-99.
95. Pääkkö, M., et al., *Enzymatic hydrolysis combined with mechanical shearing and high-pressure homogenization for nanoscale cellulose fibrils and strong gels*. Biomacromolecules, 2007. 8(6): p. 1934-1941.
96. Filson, P.B., Dawson-Andoh, B.E., and Schwegler-Berry, D.J.G.C., *Enzymatic-mediated production of cellulose nanocrystals from recycled pulp*. Green Chem., 2009. 11(11): p. 1808-1814.
97. Wang, W., et al., *Endoglucanase post-milling treatment for producing cellulose nanofibers from bleached eucalyptus fibers by a supermasscolloider*. Cellulose, 2016. 23(3): p. 1859-1870.
98. Zhu, J.Y., Sabo, R., and Luo, X.J.G.C., *Integrated production of nano-fibrillated cellulose and cellulosic biofuel (ethanol) by enzymatic fractionation of wood fibers*. Green Chem., 2011. 13(5): p. 1339-1344.
99. Tang, Y., et al., *Extraction of cellulose nano-crystals from old corrugated container fiber using phosphoric acid and enzymatic hydrolysis followed by sonication*. Carbohydr. Polym., 2015. 125: p. 360-366.

100. Anderson, S.R., et al., *Enzymatic preparation of nanocrystalline and microcrystalline cellulose*. TAPPI J., 2014. 13(5): p. 35-42.
101. Beyene, D., et al., *Characterization of cellulase-treated fibers and resulting cellulose nanocrystals generated through acid hydrolysis*. Materials, 2018. 11(8): p. 1272.
102. Satyamurthy, P., Vigneshwaran, N.J.E., and technology, m., *A novel process for synthesis of spherical nanocellulose by controlled hydrolysis of microcrystalline cellulose using anaerobic microbial consortium*. Enzyme Microb. Technol., 2013. 52(1): p. 20-25.
103. Mariño, M., et al., *Enhanced materials from nature: Nanocellulose from citrus waste*. Molecules, 2015. 20(4): p. 5908-5923.
104. George, J., Ramana, K., and Bawa, A.J.I.J.o.B.M., *Bacterial cellulose nanocrystals exhibiting high thermal stability and their polymer nanocomposites*. Int. J. Biol. Macromol., 2011. 48(1): p. 50-57.
105. Satyamurthy, P., et al., *Preparation and characterization of cellulose nanowhiskers from cotton fibres by controlled microbial hydrolysis*. Carbohydr. Polym., 2011. 83(1): p. 122-129.
106. de Campos, A., et al., *Obtaining nanofibers from curauá and sugarcane bagasse fibers using enzymatic hydrolysis followed by sonication*. Cellulose, 2013. 20(3): p. 1491-1500.
107. Heinzelman, P., et al., *A family of thermostable fungal cellulases created by structure-guided recombination*. Proc. Natl. Acad. Sci. U.S.A., 2009: p. pnas. 0901417106.
108. Privett, H.K., et al., *Iterative approach to computational enzyme design*. Proc. Natl. Acad. Sci. U.S.A., 2012.
109. Moore, J.C. and Arnold, F.H., *Directed evolution of a para-nitrobenzyl esterase for aqueous-organic solvents*. Nat. Biotechnol., 1996. 14(4): p. 458.
110. Yang, H., et al., *Evolving artificial metalloenzymes via random mutagenesis*. Nat. Chem., 2018. 10(3): p. 318.
111. Manteca, A., et al., *Mechanochemical evolution of the giant muscle protein titin as inferred from resurrected proteins*. Nat. Struct. Mol. Biol., 2017. 24(8): p. 652.
112. Risso, V.A., et al., *Hyperstability and substrate promiscuity in laboratory resurrections of precambrian β -lactamases*. J. Am. Chem. Soc., 2013. 135(8): p. 2899-2902.

113. Perez-Jimenez, R., et al., *Single-molecule paleoenzymology probes the chemistry of resurrected enzymes*. *Nat. Struct. Mol. Biol.*, 2011. 18(5): p. 592.
114. Gaucher, E.A., et al., *Inferring the palaeoenvironment of ancient bacteria on the basis of resurrected proteins*. *Nature*, 2003. 425(6955): p. 285.
115. Gumulya, Y., et al., *Engineering highly functional thermostable proteins using ancestral sequence reconstruction*. *Nat. Catal.*, 2018. 1(11): p. 878.
116. Henrissat, B., et al., *Synergism of cellulases from trichoderma reesei in the degradation of cellulose*. *Nat. Biotechnol.*, 1985. 3(8): p. 722.
117. Jørgensen, H., et al., *Enzymatic conversion of lignocellulose into fermentable sugars: Challenges and opportunities*. *Biofuel. Bioprod. Biorefin.*, 2007. 1(2): p. 119-134.
118. Hong, J., Ye, X., and Zhang, Y.-H.P.J.L., *Quantitative determination of cellulose accessibility to cellulase based on adsorption of a nonhydrolytic fusion protein containing cbm and gfp with its applications*. *Langmuir*, 2007. 23(25): p. 12535-12540.
119. Reyes-Ortiz, V., et al., *Addition of a carbohydrate-binding module enhances cellulase penetration into cellulose substrates*. *Biotechnol. Biofuels*, 2013. 6(1): p. 93.
120. Liu, Y.-S., et al., *Cellobiohydrolase hydrolyzes crystalline cellulose on hydrophobic faces*. *J. Biol. Chem.*, 2011: p. jbc.M110.216556.
121. Bayer, E.A., et al., *Cellulosomes—structure and ultrastructure*. *J. Struct. Biol.*, 1998. 124(2-3): p. 221-234.
122. Carvalho, A.L., et al., *Cellulosome assembly revealed by the crystal structure of the cohesin–dockerin complex*. *Proc. Natl. Acad. Sci. U.S.A.*, 2003. 100(24): p. 13809-13814.
123. Krauss, J., et al., *In vitro reconstitution of the complete clostridium thermocellum cellulosome and synergistic activity on crystalline cellulose*. *Appl. Environ. Microbiol.*, 2012: p. AEM.07959-11.
124. Gefen, G., et al., *Enhanced cellulose degradation by targeted integration of a cohesin-fused β -glucosidase into the clostridium thermocellum cellulosome*. *Proc. Natl. Acad. Sci. U.S.A.*, 2012. 109(26): p. 10298-10303.

125. Busk, P.K. and Lange, L., *Classification of fungal and bacterial lytic polysaccharide monooxygenases*. BMC genomics, 2015. 16(1): p. 368.
126. Chiu, E., et al., *Structural basis for the enhancement of virulence by viral spindles and their in vivo crystallization*. Proc. Natl. Acad. Sci. U.S.A., 2015: p. 201418798.
127. Vaaje-Kolstad, G., et al., *An oxidative enzyme boosting the enzymatic conversion of recalcitrant polysaccharides*. Science, 2010. 330(6001): p. 219-222.
128. Quinlan, R.J., et al., *Insights into the oxidative degradation of cellulose by a copper metalloenzyme that exploits biomass components*. Proc. Natl. Acad. Sci. U.S.A., 2011. 108(37): p. 15079-15084.
129. Agger, J.W., et al., *Discovery of lpmo activity on hemicelluloses shows the importance of oxidative processes in plant cell wall degradation*. Proc. Natl. Acad. Sci. U.S.A., 2014: p. 201323629.
130. Leggio, L.L., et al., *Structure and boosting activity of a starch-degrading lytic polysaccharide monooxygenase*. Nat. Commun., 2015. 6: p. 5961.
131. Phillips, C.M., et al., *Cellobiose dehydrogenase and a copper-dependent polysaccharide monooxygenase potentiate cellulose degradation by neurospora crassa*. ACS Chem. Biol., 2011. 6(12): p. 1399-1406.
132. Beeson, W.T., et al., *Oxidative cleavage of cellulose by fungal copper-dependent polysaccharide monooxygenases*. J. Am. Chem. Soc., 2011. 134(2): p. 890-892.
133. Forsberg, Z., et al., *Structural and functional characterization of a conserved pair of bacterial cellulose-oxidizing lytic polysaccharide monooxygenases*. Proc. Natl. Acad. Sci. U.S.A., 2014. 111(23): p. 8446-8451.
134. Forsberg, Z., et al., *Comparative study of two chitin-active and two cellulose-active aa10-type lytic polysaccharide monooxygenases*. Biochemistry, 2014. 53(10): p. 1647-1656.
135. Vu, V.V., et al., *Determinants of regioselective hydroxylation in the fungal polysaccharide monooxygenases*. J. Am. Chem. Soc., 2013. 136(2): p. 562-565.
136. Cannella, D., et al., *Production and effect of aldonic acids during enzymatic hydrolysis of lignocellulose at high dry matter content*. Biotechnol. Biofuels, 2012. 5(1): p. 26.

137. Müller, G., et al., *The impact of hydrogen peroxide supply on lpmo activity and overall saccharification efficiency of a commercial cellulase cocktail*. *Biotechnol. Biofuels*, 2018. 11(1): p. 209.
138. Arfi, Y., et al., *Integration of bacterial lytic polysaccharide monoxygenases into designer cellulosomes promotes enhanced cellulose degradation*. *Proc. Natl. Acad. Sci. U.S.A.*, 2014. 111(25): p. 9109-9114.
139. Dimarogona, M., Topakas, E., and Christakopoulos, P., *Recalcitrant polysaccharide degradation by novel oxidative biocatalysts*. *Appl. Microbiol. Biotechnol.*, 2013. 97(19): p. 8455-8465.
140. Saha, B.C., *Hemicellulose bioconversion*. *J. Ind. Microbiol. Biotechnol.*, 2003. 30(5): p. 279-291.
141. Vanholme, R., et al., *Lignin biosynthesis and structure*. *Plant Physiol.*, 2010. 153(3): p. 895-905.
142. Mood, S.H., et al., *Lignocellulosic biomass to bioethanol, a comprehensive review with a focus on pretreatment*. *Renew. Sust. Energ. Rev.*, 2013. 27: p. 77-93.
143. Gírio, F.M., et al., *Hemicelluloses for fuel ethanol: A review*. *Bioresour. Technol.*, 2010. 101(13): p. 4775-4800.
144. Carpita, N.C. and Gibeaut, D.M., *Structural models of primary cell walls in flowering plants: Consistency of molecular structure with the physical properties of the walls during growth*. *Plant J.*, 1993. 3(1): p. 1-30.
145. Chundawat, S.P., et al., *Deconstruction of lignocellulosic biomass to fuels and chemicals*. *Annu. Rev. Chem. Biomol. Eng.*, 2011.
146. Esteghlalian, A., et al., *Modeling and optimization of the dilute-sulfuric-acid pretreatment of corn stover, poplar and switchgrass*. *Bioresour. Technol.*, 1997. 59(2-3): p. 129-136.
147. Cheng, Y.-S., et al., *Evaluation of high solids alkaline pretreatment of rice straw*. *Appl. Biochem. Biotechnol.*, 2010. 162(6): p. 1768-1784.
148. Rabemanolontsoa, H. and Saka, S., *Various pretreatments of lignocellulosics*. *Bioresour. Technol.*, 2016. 199: p. 83-91.
149. Yachmenev, V., et al., *Acceleration of the enzymatic hydrolysis of corn stover and sugar cane bagasse celluloses by low intensity uniform ultrasound*. *J. Biobased Mater. Bio.*, 2009. 3(1): p. 25-31.

150. Wong, K., Tan, L., and Saddler, J.N., *Multiplicity of beta-1, 4-xylanase in microorganisms: Functions and applications*. Microbiol. Rev., 1988. 52(3): p. 305.
151. Madlala, A.M., et al., *Xylanase-induced reduction of chlorine dioxide consumption during elemental chlorine-free bleaching of different pulp types*. Biotechnol. Lett., 2001. 23(5): p. 345-351.
152. Battan, B., et al., *Enhanced production of cellulase-free thermostable xylanase by bacillus pumilus ash and its potential application in paper industry*. Enzyme Microb. Technol., 2007. 41(6-7): p. 733-739.
153. Laureano-Perez, L., et al., *Understanding factors that limit enzymatic hydrolysis of biomass*. Appl. Biochem. Biotechnol., 2005. 124(1-3): p. 1081-1099.
154. Öhgren, K., et al., *Effect of hemicellulose and lignin removal on enzymatic hydrolysis of steam pretreated corn stover*. Bioresour. Technol., 2007. 98(13): p. 2503-2510.
155. Sathitsuksanoh, N., et al., *Lignin fate and characterization during ionic liquid biomass pretreatment for renewable chemicals and fuels production*. Green Chem., 2014. 16(3): p. 1236-1247.
156. Heinzkill, M., et al., *Characterization of laccases and peroxidases from wood-rotting fungi (family coprinaceae)*. Appl. Environ. Microbiol., 1998. 64(5): p. 1601-1606.
157. Arias, M.E., et al., *Kraft pulp biobleaching and mediated oxidation of a nonphenolic substrate by laccase from streptomyces cyaneus cect 3335*. Appl. Environ. Microbiol., 2003. 69(4): p. 1953-1958.
158. Barruetabeña, N., *Ancestral sequence reconstruction for protein engineering: Improving celulasas for biomass hydrolysis*, 2017, UPV/EHU.
159. Cells, A.T.X.-B.C., [Http://www.Chem-agilent.Com/pdf/strata/200249.Pdf](http://www.Chem-agilent.Com/pdf/strata/200249.Pdf).
160. Azam, A., et al., *Type iii secretion as a generalizable strategy for the production of full-length biopolymer-forming proteins*. Biotechnol Bioeng, 2016. 113(11): p. 2313-20.
161. Glasgow, J.E., et al., *Influence of electrostatics on small molecule flux through a protein nanoreactor*. ACS Synth Biol, 2015. 4(9): p. 1011-9.
162. Kim, E.Y., Jakobson, C.M., and Tullman-Ercek, D., *Engineering transcriptional regulation to control pdu*

- microcompartment formation*. PLoS One, 2014. 9(11): p. e113814.
163. Marsden, W.L., et al., *Evaluation of the dns method for analysing lignocellulosic hydrolysates*. J. Chem. Technol. Biotechnol., 1982. 32(7-12): p. 1016-1022.
164. Miller, G.L.J.A.c., *Use of dinitrosalicylic acid reagent for determination of reducing sugar*. Anal. Chem., 1959. 31(3): p. 426-428.
165. Mandels, M. and Sternberg, D.J.J.F.T., *Recent advances in cellulase technology*. J. Ferment. Technol., 1976. 54(4): p. 267-286.
166. Dong, X.M., Revol, J.-F., and Gray, D.G., *Effect of microcrystallite preparation conditions on the formation of colloid crystals of cellulose*. Cellulose, 1998. 5(1): p. 19-32.
167. Segal, L., et al., *An empirical method for estimating the degree of crystallinity of native cellulose using the x-ray diffractometer*. Text. Res. J., 1959. 29(10): p. 786-794.
168. Cullity, B.D., *Elements of x-ray diffraction*. Wesley Mass, 1978.
169. Costa, M.N., et al., *A low cost, safe, disposable, rapid and self-sustainable paper-based platform for diagnostic testing: Lab-on-paper*. Nanotechnology, 2014. 25(9): p. 094006.
170. MacKay, R.M., et al., *Structure of a bacillus subtilis endo- β -1,4-glucanase gene*. Nucleic Acids Res., 1986. 14(22): p. 9159-9170.
171. Li, Y., Irwin, D.C., and Wilson, D.B., *Processivity, substrate binding, and mechanism of cellulose hydrolysis by thermobifida fusca cel9a*. Appl. Microbiol. Biotechnol., 2007. 73(10): p. 3165-72.
172. Pereira, J.H., et al., *Biochemical characterization and crystal structure of endoglucanase cel5a from the hyperthermophilic thermotoga maritima*. J. Struct. Biol., 2010. 172(3): p. 372-9.
173. Reid, M.S., et al., *Effect of ionic strength and surface charge density on the kinetics of cellulose nanocrystal thin film swelling*. Langmuir, 2017. 33(30): p. 7403-7411.
174. Tang, Y., et al., *Preparation and characterization of nanocrystalline cellulose via low-intensity ultrasonic-assisted sulfuric acid hydrolysis*. Cellulose, 2014. 21(1): p. 335-346.
175. Sato, Y., Kusaka, Y., and Kobayashi, M., *Charging and aggregation behavior of cellulose nanofibers in aqueous solution*. Langmuir, 2017. 33(44): p. 12660-12669.

176. Le Costaouëc, T., et al., *The role of carbohydrate binding module (cbm) at high substrate consistency: Comparison of trichoderma reesei and thermoascus aurantiacus cel7a (cbhi) and cel5a (egii)*. Bioresour. Technol., 2013. 143: p. 196-203.
177. Liu, W., et al., *Engineering of clostridium phytofermentans endoglucanase cel5a for improved thermostability*. Appl. Environ. Microbiol., 2010. 76(14): p. 4914-4917.
178. Chhabra, S.R., et al., *Regulation of endo-acting glycosyl hydrolases in the hyperthermophilic bacterium thermotoga maritima grown on glucan-and mannan-based polysaccharides*. Appl. Environ. Microbiol., 2002. 68(2): p. 545-554.
179. Mandal, A. and Chakrabarty, D.J.C.P., *Isolation of nanocellulose from waste sugarcane bagasse (scb) and its characterization*. Carbohydr. Polym., 2011. 86(3): p. 1291-1299.
180. Yarbrough, J.M., et al., *Multifunctional cellulolytic enzymes outperform processive fungal cellulases for coproduction of nanocellulose and biofuels*. Acs Nano, 2017. 11(3): p. 3101-3109.
181. Ya-Yu Li, B.W., Ming-Guo Ma, and Bo Wang, *The influence of pre-treatment time and sulfuric acid on cellulose nanocrystals*. Bioresources 2018. 13(2): p. 3585-3602.
182. Chakraborty, A., Sain, M., and Kortschot, M., *Cellulose microfibrils: A novel method of preparation using high shear refining and cryocrushing*. Holzforschung, 2005. 59(1): p. 102-107.
183. Pranger, L. and Tannenbaum, R., *Biobased nanocomposites prepared by in situ polymerization of furfuryl alcohol with cellulose whiskers or montmorillonite clay*. Macromolecules, 2008. 41(22): p. 8682-8687.
184. de Rodriguez, N.L.G., Thielemans, W., and Dufresne, A., *Sisal cellulose whiskers reinforced polyvinyl acetate nanocomposites*. Cellulose, 2006. 13(3): p. 261-270.
185. Cherhal, F., Cousin, F., and Capron, I., *Influence of charge density and ionic strength on the aggregation process of cellulose nanocrystals in aqueous suspension, as revealed by small-angle neutron scattering*. Langmuir, 2015. 31(20): p. 5596-5602.
186. de Souza Lima, M.M. and Borsali, R., *Rodlike cellulose microcrystals: Structure, properties, and applications*. Macromol. Rapid Commun., 2004. 25(7): p. 771-787.

187. Sèbe, G., et al., *Supramolecular structure characterization of cellulose ii nanowhiskers produced by acid hydrolysis of cellulose i substrates*. *Biomacromolecules*, 2012. 13(2): p. 570-578.
188. Kurašin, M. and Väljamäe, P., *Processivity of cellobiohydrolases is limited by the substrate*. *J. Biol. Chem.*, 2011. 286(1): p. 169-177.
189. Zhang, K.-D., et al., *Processive degradation of crystalline cellulose by a multimodular endoglucanase via a wirewalking mode*. *Biomacromolecules*, 2018. 19(5): p. 1686-1696.
190. Adel, A.M., et al., *Characterization of microcrystalline cellulose prepared from lignocellulosic materials. Part ii: Physicochemical properties*. *Carbohydr. Polym.*, 2011. 83(2): p. 676-687.
191. Guo, X., et al., *Qualitatively and quantitatively characterizing water adsorption of a cellulose nanofiber film using micro-ftir spectroscopy*. *RSC Adv.*, 2018. 8(8): p. 4214-4220.
192. Åkerholm, M., Hinterstoisser, B., and Salmén, L., *Characterization of the crystalline structure of cellulose using static and dynamic ft-ir spectroscopy*. *Carbohydr. Polym.*, 2004. 339(3): p. 569-578.
193. Bouchard, J., et al., *Characterization of depolymerized cellulosic residues*. *Wood Sci. Technol.*, 1990. 24(2): p. 159-169.
194. Poletto, M., Ornaghi, H.L., and Zattera, A.J., *Native cellulose: Structure, characterization and thermal properties*. *Materials*, 2014. 7(9): p. 6105-6119.
195. Lee, C.M., et al., *Cellulose polymorphism study with sum-frequency-generation (sfg) vibration spectroscopy: Identification of exocyclic ch 2 oh conformation and chain orientation*. *Cellulose*, 2013. 20(3): p. 991-1000.
196. Dai, J., et al., *Co-production of cellulose nanocrystals and fermentable sugars assisted by endoglucanase treatment of wood pulp*. *Materials*, 2018. 11(9): p. 1645.
197. Susi, H. and Byler, D.M., *Resolution-enhanced fourier transform infrared spectroscopy of enzymes*, in *Meth. Enzymol.* 1986, Elsevier. p. 290-311.
198. Imai, T. and Sugiyama, J., *Nanodomains of α and β cellulose in algal microfibrils*. *Macromolecules*, 1998. 31(18): p. 6275-6279.

199. Han, J., et al., *Self-assembling behavior of cellulose nanoparticles during freeze-drying: Effect of suspension concentration, particle size, crystal structure, and surface charge*. *Biomacromolecules*, 2013. 14(5): p. 1529-1540.
200. Gwon, J.G., et al., *Characterization of chemically modified wood fibers using ftir spectroscopy for biocomposites*. *J. Appl. Polym. Sci.*, 2010. 116(6): p. 3212-3219.
201. Oh, S.Y., et al., *Crystalline structure analysis of cellulose treated with sodium hydroxide and carbon dioxide by means of x-ray diffraction and ftir spectroscopy*. *Carbohydr. Res.*, 2005. 340(15): p. 2376-2391.
202. Dhar, P., et al., *Effect of cellulose nanocrystal polymorphs on mechanical, barrier and thermal properties of poly (lactic acid) based bionanocomposites*. *RSC Adv.*, 2015. 5(74): p. 60426-60440.
203. Xie, Y.L., Wang, M.J., and Yao, S.J., *Preparation and characterization of biocompatible microcapsules of sodium cellulose sulfate/chitosan by means of layer-by-layer self-assembly*. *Langmuir*, 2009. 25(16): p. 8999-9005.
204. Dinand, E., et al., *Mercerization of primary wall cellulose and its implication for the conversion of cellulose i→ cellulose ii*. *Cellulose*, 2002. 9(1): p. 7-18.
205. Liu, X., et al., *Effects of hydrophilic fillers on the thermal degradation of poly (lactic acid)*. *Thermochimica Acta*, 2010. 509(1-2): p. 147-151.
206. Huth, F., et al., *Nano-ftir absorption spectroscopy of molecular fingerprints at 20 nm spatial resolution*. *Nano Lett.*, 2012. 12(8): p. 3973-3978.
207. Ugarte, L., et al., *An alternative approach for the incorporation of cellulose nanocrystals in flexible polyurethane foams based on renewably sourced polyols*. *Ind. Crops. Prod.*, 2017. 95: p. 564-573.
208. Lin, N. and Dufresne, A., *Surface chemistry, morphological analysis and properties of cellulose nanocrystals with gradiented sulfation degrees*. *Nanoscale*, 2014. 6(10): p. 5384-5393.
209. Abitbol, T., et al., *Surface charge influence on the phase separation and viscosity of cellulose nanocrystals*. *Langmuir*, 2018. 34(13): p. 3925-3933.
210. Liu, Y. and Hu, H., *X-ray diffraction study of bamboo fibers treated with naoh*. *Fibers. Polym.*, 2008. 9(6): p. 735-739.

211. Qian, S., Zhang, H., and Sheng, K., *Cellulose nanowhiskers from moso bamboo residues: Extraction and characterization*. *BioResources*, 2016. 12(1): p. 419-433.
212. Ciolacu, D., et al., *Enzymatic hydrolysis of different allomorphic forms of microcrystalline cellulose*. *Cellulose*, 2011. 18(6): p. 1527-1541.
213. Mahadeva, S.K. and Kim, J., *Electromechanical behavior of room temperature ionic liquid dispersed cellulose*. *J. Phys. Chem. C*, 2009. 113(28): p. 12523-12529.
214. Zuluaga, R., et al., *Cellulose microfibrils from banana rachis: Effect of alkaline treatments on structural and morphological features*. *Carbohydr. Polym.*, 2009. 76(1): p. 51-59.
215. Lee, C., et al., *Correlations of apparent cellulose crystallinity determined by xrd, nmr, ir, raman, and sfg methods, in Cellulose chemistry and properties: Fibers, nanocelluloses and advanced materials*. 2015, Springer. p. 115-131.
216. Peng, Y., et al., *Influence of drying method on the material properties of nanocellulose i: Thermostability and crystallinity*. *Cellulose*, 2013. 20(5): p. 2379-2392.
217. Xiao, Z., et al., *Cellulose-binding domain of endoglucanase iii from trichoderma reesei disrupting the structure of cellulose*. *Biotechnol. Lett.*, 2001. 23(9): p. 711-715.
218. Yue, Y., et al., *Comparative properties of cellulose nanocrystals from native and mercerized cotton fibers*. *Cellulose*, 2012. 19(4): p. 1173-1187.
219. Elazzouzi-Hafraoui, S., et al., *The shape and size distribution of crystalline nanoparticles prepared by acid hydrolysis of native cellulose*. *Biomacromolecules*, 2007. 9(1): p. 57-65.
220. Gong, J., et al., *Research on cellulose nanocrystals produced from cellulose sources with various polymorphs*. *RSC Adv.*, 2017. 7(53): p. 33486-33493.
221. Xing, L., et al., *Cellulose i and ii nanocrystals produced by sulfuric acid hydrolysis of tetra pak cellulose i*. *Carbohydr. Polym.*, 2018. 192: p. 184-192.
222. Kono, H., et al., *Cp/mas 13c nmr study of cellulose and cellulose derivatives. 1. Complete assignment of the cp/mas 13c nmr spectrum of the native cellulose*. *J. Am. Chem. Soc.*, 2002. 124(25): p. 7506-7511.
223. Isogai, A., et al., *Solid-state cp/mas carbon-13 nmr study of cellulose polymorphs*. *Macromolecules*, 1989. 22(7): p. 3168-3172.

224. Newman, R.H., *Estimation of the lateral dimensions of cellulose crystallites using ^{13}C nmr signal strengths*. *Solid State Nucl. Magn. Reson.*, 1999. 15(1): p. 21-29.
225. Sacui, I.A., et al., *Comparison of the properties of cellulose nanocrystals and cellulose nanofibrils isolated from bacteria, tunicate, and wood processed using acid, enzymatic, mechanical, and oxidative methods*. *ACS Appl. Mater. Interfaces*, 2014. 6(9): p. 6127-6138.
226. Atalla, R.H., et al., *Carbon-13 nmr spectra of cellulose polymorphs*. *J. Am. Chem. Soc.*, 1980. 102(9): p. 3249-3251.
227. Lee, K.-Y., et al., *High performance cellulose nanocomposites: Comparing the reinforcing ability of bacterial cellulose and nanofibrillated cellulose*. *ACS Appl. Mater. Interfaces*, 2012. 4(8): p. 4078-4086.
228. Morteza Mostashari, S. and Fallah Moafi, H., *Thermogravimetric analysis of a cellulosic fabric incorporated with ammonium iron (ii)-sulfate hexahydrate as a flame-retardant*. *J. Ind. Text.*, 2007. 37(1): p. 31-42.
229. Henriksson, G., Christiernin, M., and Agnemo, R., *Monocomponent endoglucanase treatment increases the reactivity of softwood sulphite dissolving pulp*. *J. Ind. Microbiol. Biotechnol.*, 2005. 32(5): p. 211-214.
230. Matsuoka, S., Kawamoto, H., and Saka, S., *Thermal glycosylation and degradation reactions occurring at the reducing ends of cellulose during low-temperature pyrolysis*. *Carbohydr. Res.*, 2011. 346(2): p. 272-279.
231. Gong, J., Mo, L., and Li, J., *A comparative study on the preparation and characterization of cellulose nanocrystals with various polymorphs*. *Carbohydr. Polym.*, 2018. 195: p. 18-28.
232. Wang, N., Ding, E., and Cheng, R., *Thermal degradation behaviors of spherical cellulose nanocrystals with sulfate groups*. *Polymer*, 2007. 48(12): p. 3486-3493.
233. Requejo, A., et al., *Tcf bleaching sequence in kraft pulping of olive tree pruning residues*. *Bioresour. Technol.*, 2012. 117: p. 117-123.
234. Da Silva, T.A., et al., *Chemical characterization of pulp components in unbleached softwood kraft fibers recycled with the assistance of a laccase/hbt system*. *BioResources*, 2007. 2(4): p. 616-629.

235. Gellerstedt, G. and Lindfors, E.-L., *Structural changes in lignin during kraft pulping*. *Holzforschung*, 1984. 38(3): p. 151-158.
236. Hu, J., et al., *Enzyme mediated nanofibrillation of cellulose by the synergistic actions of an endoglucanase, lytic polysaccharide monooxygenase (lpmo) and xylanase*. *Sci. Rep.*, 2018. 8(1): p. 3195.
237. Paice, M.G., et al., *A xylanase gene from bacillus subtilis: Nucleotide sequence and comparison with b. Pumilus gene*. *Arch. Microbiol.*, 1986. 144(3): p. 201-206.
238. Ramachandran, S., Magnuson, T.S., and Crawford, D.L., *Cloning, sequencing, and characterization of two clustered cellulase-encoding genes, cels1 and cels2, from streptomyces viridosporus t7a and their expression in escherichia coli*. *Actinomycetologica*, 2000. 14(1): p. 11-16.
239. Várnai, A., Siika-aho, M., and Viikari, L., *Restriction of the enzymatic hydrolysis of steam-pretreated spruce by lignin and hemicellulose*. *Enzyme Microb. Technol.*, 2010. 46(3-4): p. 185-193.
240. Kumar, R. and Wyman, C.E., *Effect of xylanase supplementation of cellulase on digestion of corn stover solids prepared by leading pretreatment technologies*. *Bioresour. Technol.*, 2009. 100(18): p. 4203-4213.
241. Hu, J., Arantes, V., and Saddler, J.N., *The enhancement of enzymatic hydrolysis of lignocellulosic substrates by the addition of accessory enzymes such as xylanase: Is it an additive or synergistic effect?* *Biotechnol. Biofuels*, 2011. 4(1): p. 36.
242. Penttilä, P.A., et al., *Xylan as limiting factor in enzymatic hydrolysis of nanocellulose*. *Bioresour. Technol.*, 2013. 129: p. 135-141.
243. Karnaouri, A., et al., *Recombinant expression of thermostable processive mt eg5 endoglucanase and its synergism with mt lpmo from myceliophthora thermophila during the hydrolysis of lignocellulosic substrates*. *Biotechnol. Biofuels*, 2017. 10(1): p. 126.
244. Sabbadin, F., et al., *An ancient family of lytic polysaccharide monooxygenases with roles in arthropod development and biomass digestion*. *Nat. Commun.*, 2018. 9(1): p. 756.

245. Rodríguez-Zúñiga, U.F., et al., *Lignocellulose pretreatment technologies affect the level of enzymatic cellulose oxidation by lpmo*. *Green Chem.*, 2015. 17(5): p. 2896-2903.
246. Jung, S., et al., *Enhanced lignocellulosic biomass hydrolysis by oxidative lytic polysaccharide monoxygenases (lpms) gh61 from gloeophyllum trabeum*. *Enzyme Microb. Technol.*, 2015. 77: p. 38-45.
247. Saelee, K., et al., *An environmentally friendly xylanase-assisted pretreatment for cellulose nanofibrils isolation from sugarcane bagasse by high-pressure homogenization*. *Ind. Crops. Prod.*, 2016. 82: p. 149-160.
248. Long, L., et al., *A xylanase-aided enzymatic pretreatment facilitates cellulose nanofibrillation*. *Bioresour. Technol.*, 2017. 243: p. 898-904.
249. Villares, A., et al., *Lytic polysaccharide monoxygenases disrupt the cellulose fibers structure*. *Sci. Rep.*, 2017. 7: p. 40262.
250. Xu, Q., et al., *Nanocrystalline cellulose from aspen kraft pulp and its application in deinked pulp*. *Int. J. Biol. Macromol.*, 2013. 60: p. 241-247.
251. Jin, L., et al., *Cellulose nanofibers prepared from tempoxidation of kraft pulp and its flocculation effect on kaolin clay*. *J. Appl. Polym. Sci.*, 2014. 131(12).
252. Sharma, P., et al., *An eco-friendly process for biobleaching of eucalyptus kraft pulp with xylanase producing bacillus halodurans*. *J. Clean Prod.*, 2015. 87: p. 966-970.
253. Coseri, S., et al., *One-shot carboxylation of microcrystalline cellulose in the presence of nitroxyl radicals and sodium periodate*. *RSC Adv.*, 2015. 5(104): p. 85889-85897.
254. Zhou, J.-H., et al., *Characterization of surface oxygen complexes on carbon nanofibers by tpd, xps and ft-ir*. *Carbon*, 2007. 45(4): p. 785-796.
255. Jiang, F., Han, S., and Hsieh, Y.-L., *Controlled defibrillation of rice straw cellulose and self-assembly of cellulose nanofibrils into highly crystalline fibrous materials*. *RSC Adv.*, 2013. 3(30): p. 12366-12375.
256. Fujisawa, S., et al., *Preparation and characterization of tempoxidized cellulose nanofibril films with free carboxyl groups*. *Carbohydr. Polym.*, 2011. 84(1): p. 579-583.

257. Ju, X., et al., *An improved x-ray diffraction method for cellulose crystallinity measurement*. Carbohydr. Polym., 2015. 123: p. 476-481.
258. Cao, Y. and Tan, H., *Study on crystal structures of enzyme-hydrolyzed cellulosic materials by x-ray diffraction*. Enzyme Microb. Technol., 2005. 36(2-3): p. 314-317.
259. Zhang, K., et al., *Extraction and comparison of carboxylated cellulose nanocrystals from bleached sugarcane bagasse pulp using two different oxidation methods*. Carbohydr. Polym., 2016. 138: p. 237-243.
260. Kafle, K., et al., *Effects of delignification on crystalline cellulose in lignocellulose biomass characterized by vibrational sum frequency generation spectroscopy and x-ray diffraction*. Bioenergy Res., 2015. 8(4): p. 1750-1758.
261. Yang, H., et al., *Characteristics of hemicellulose, cellulose and lignin pyrolysis*. Fuel, 2007. 86(12-13): p. 1781-1788.
262. Saito, T., et al., *Homogeneous suspensions of individualized microfibrils from tempo-catalyzed oxidation of native cellulose*. Biomacromolecules, 2006. 7(6): p. 1687-1691.
263. Gomez-Bujedo, S., Fleury, E., and Vignon, M.R., *Preparation of cellouronic acids and partially acetylated cellouronic acids by tempo/naclO oxidation of water-soluble cellulose acetate*. Biomacromolecules, 2004. 5(2): p. 565-571.
264. Zhao, J., et al., *Thermal degradation of softwood lignin and hardwood lignin by tg-ftir and py-gc/ms*. Polym. Degrad. Stab., 2014. 108: p. 133-138.
265. Lin, N., et al., *Surface acetylation of cellulose nanocrystal and its reinforcing function in poly (lactic acid)*. Carbohydr. Polym., 2011. 83(4): p. 1834-1842.
266. Cao, X., Dong, H., and Li, C.M., *New nanocomposite materials reinforced with flax cellulose nanocrystals in waterborne polyurethane*. Biomacromolecules, 2007. 8(3): p. 899-904.
267. Naduparambath, S., et al., *Isolation and characterisation of cellulose nanocrystals from sago seed shells*. Carbohydr. Polym., 2018. 180: p. 13-20.
268. Lei, W., et al., *Polyurethane elastomer composites reinforced with waste natural cellulosic fibers from office paper in thermal properties*. Carbohydr. Polym., 2018.
269. Tien, Y. and Wei, K., *High-tensile-property layered silicates/polyurethane nanocomposites by using reactive*

- silicates as pseudo chain extenders*. *Macromolecules*, 2001. 34(26): p. 9045-9052.
270. Pei, A., et al., *Strong nanocomposite reinforcement effects in polyurethane elastomer with low volume fraction of cellulose nanocrystals*. *Macromolecules*, 2011. 44(11): p. 4422-4427.
271. Kong, X., Zhao, L., and Curtis, J.M., *Polyurethane nanocomposites incorporating biobased polyols and reinforced with a low fraction of cellulose nanocrystals*. *Carbohydr. Polym.*, 2016. 152: p. 487-495.
272. Lei, W., et al., *Eco-friendly waterborne polyurethane reinforced with cellulose nanocrystal from office waste paper by two different methods*. *Carbohydr. Polym.*, 2019.
273. Shin, E., Choi, S., and Lee, J., *Fabrication of regenerated cellulose nanoparticles/waterborne polyurethane nanocomposites*. *J. Appl. Polym. Sci.*, 2018. 135(35): p. 46633.
274. Wu, Q., et al., *A high strength nanocomposite based on microcrystalline cellulose and polyurethane*. *Biomacromolecules*, 2007. 8(12): p. 3687-3692.
275. Santamaria-Echart, A., et al., *Waterborne polyurethane-urea dispersion with chain extension step in homogeneous medium reinforced with cellulose nanocrystals*. *Compos. B. Eng.*, 2018. 137: p. 31-38.
276. Saralegi, A., et al., *From elastomeric to rigid polyurethane/cellulose nanocrystal bionanocomposites*. *Compos. Sci. Technol.*, 2013. 88: p. 39-47.
277. de Oliveira Patricio, P.S., et al., *Tailoring the morphology and properties of waterborne polyurethanes by the procedure of cellulose nanocrystal incorporation*. *Eur. Polym. J.*, 2013. 49(12): p. 3761-3769.
278. Siqueira, G., Bras, J., and Dufresne, A., *Cellulose whiskers versus microfibrils: Influence of the nature of the nanoparticle and its surface functionalization on the thermal and mechanical properties of nanocomposites*. *Biomacromolecules*, 2008. 10(2): p. 425-432.
279. Sun, X., et al., *Surface wetting behavior of nanocellulose-based composite films*. *Cellulose*, 2018. 25(9): p. 5071-5087.
280. Ljungberg, N., et al., *New nanocomposite materials reinforced with cellulose whiskers in atactic polypropylene: Effect of surface and dispersion characteristics*. *Biomacromolecules*, 2005. 6(5): p. 2732-2739.

281. Chang, P.R., et al., *Preparation and properties of glycerol plasticized-starch (gps)/cellulose nanoparticle (cn) composites*. Carbohydr. Polym., 2010. 79(2): p. 301-305.
282. Malinen, M.M., et al., *Differentiation of liver progenitor cell line to functional organotypic cultures in 3d nanofibrillar cellulose and hyaluronan-gelatin hydrogels*. Biomaterials, 2014. 35(19): p. 5110-5121.
283. Henriksson, M., et al., *Cellulose nanopaper structures of high toughness*. Biomacromolecules, 2008. 9(6): p. 1579-1585.
284. Zhang, J., et al., *Reduction of graphene oxide via l-ascorbic acid*. Chem. Commun., 2010. 46(7): p. 1112-1114.
285. Park, S., et al., *Graphene oxide papers modified by divalent ions—enhancing mechanical properties via chemical cross-linking*. ACS Nano, 2008. 2(3): p. 572-578.
286. Feng, Y., et al., *A mechanically strong, flexible and conductive film based on bacterial cellulose/graphene nanocomposite*. Carbohydr. Polym., 2012. 87(1): p. 644-649.
287. Beeran, Y., et al., *Mechanically strong, flexible and thermally stable graphene oxide/nanocellulosic films with enhanced dielectric properties*. RSC Adv., 2016. 6(54): p. 49138-49149.
288. Yang, W., et al., *Ultrathin flexible reduced graphene oxide/cellulose nanofiber composite films with strongly anisotropic thermal conductivity and efficient electromagnetic interference shielding*. J. Mater. Chem., 2017. 5(15): p. 3748-3756.
289. Kim, C.-J., et al., *Graphene oxide/cellulose composite using nmno monohydrate*. Carbohydr. Polym., 2011. 86(2): p. 903-909.
290. Mahmoudian, S., et al., *A facile approach to prepare regenerated cellulose/graphene nanoplatelets nanocomposite using room-temperature ionic liquid*. J. Nanosci. Nanotechnol., 2012. 12(7): p. 5233-5239.
291. Rivkin, A., et al., *Bionanocomposite films from resilin-cbd bound to cellulose nanocrystals*. Ind. Biotechnol., 2015. 11(1): p. 44-58.
292. Wang, F. and Drzal, L.T., *The use of cellulose nanofibrils to enhance the mechanical properties of graphene nanoplatelets papers with high electrical conductivity*. Ind. Crops. Prod., 2018. 124: p. 519-529.

293. Jiang, Q., et al., *An in situ grown bacterial nanocellulose/graphene oxide composite for flexible supercapacitors*. *J. Mater. Chem.*, 2017. 5(27): p. 13976-13982.
294. Kim, K.S., et al., *Large-scale pattern growth of graphene films for stretchable transparent electrodes*. *Nature*, 2009. 457(7230): p. 706.
295. Bae, S., et al., *Roll-to-roll production of 30-inch graphene films for transparent electrodes*. *Nat. Nanotechnol*, 2010. 5(8): p. 574.
296. Pham, V.P., et al., *Low damage pre-doping on cvd graphene/cu using a chlorine inductively coupled plasma*. *Carbon*, 2015. 95: p. 664-671.
297. Luo, Z., et al., *Effect of substrate roughness and feedstock concentration on growth of wafer-scale graphene at atmospheric pressure*. *Chem. Mater.*, 2011. 23(6): p. 1441-1447.
298. Lee, J.-K., Park, C.-S., and Kim, H., *Sheet resistance variation of graphene grown on annealed and mechanically polished cu films*. *RSC Adv.*, 2014. 4(107): p. 62453-62456.
299. García, A., et al., *Industrial and crop wastes: A new source for nanocellulose biorefinery*. *Ind. Crops Prod.*, 2016. 93: p. 26-38.
300. Alftrén, J., Hobley, T.J.J.B., and Bioenergy, *Immobilization of cellulase mixtures on magnetic particles for hydrolysis of lignocellulose and ease of recycling*. *Biomass Bioenergy*, 2014. 65: p. 72-78.
301. Jordan, J., Theegala, C.J.B.C., and Biorefinery, *Probing the limitations for recycling cellulase enzymes immobilized on iron oxide (fe 3 o 4) nanoparticles*. *Biomass Convers. Biorefin.* , 2014. 4(1): p. 25-33.
302. Gu, Y., et al., *Advances and prospects of bacillus subtilis cellular factories: From rational design to industrial applications*. *Metab. Eng.*, 2018.
303. Paloheimo, M., et al., *Production of industrial enzymes in trichoderma reesei*, in *Gene expression systems in fungi: Advancements and applications*. 2016, Springer. p. 23-57.
304. Yue, Y., *A comparative study of cellulose i and ii and fibers and nanocrystals*. 2011.
305. Isogai, A., Saito, T., and Fukuzumi, H.J.n., *Tempo-oxidized cellulose nanofibers*. *Nanoscale*, 2011. 3(1): p. 71-85.

306. Coseri, S., et al., *Oxidized cellulose—survey of the most recent achievements*. Carbohydr. Polym., 2013. 93(1): p. 207-215.
307. Kachkarova-Sorokina, S.L., Gallezot, P., and Sorokin, A.B.J.C.c., *A novel clean catalytic method for waste-free modification of polysaccharides by oxidation*. 2004(24): p. 2844-2845.
308. Karim, Z., et al., *In situ tempo surface functionalization of nanocellulose membranes for enhanced adsorption of metal ions from aqueous medium*. RSC Adv., 2017. 7(9): p. 5232-5241.
309. Dias, G., Peplow, P., and Teixeira, F.J.J.o.M.S.M.i.M., *Osseous regeneration in the presence of oxidized cellulose and collagen*. J. Mater. Sci. Mater. Med., 2003. 14(9): p. 739-745.
310. Zander, N.E., et al., *Metal cation cross-linked nanocellulose hydrogels as tissue engineering substrates*. ACS Appl. Mater. Interfaces, 2014. 6(21): p. 18502-18510.
311. Weishaupt, R., et al., *Tempo-oxidized nanofibrillated cellulose as a high density carrier for bioactive molecules*. Biomacromolecules, 2015. 16(11): p. 3640-3650.
312. Zhao, X., et al., *Biomass recalcitrance. Part i: The chemical compositions and physical structures affecting the enzymatic hydrolysis of lignocellulose*. Biofuel Bioprod, Biorefin., 2012. 6(4): p. 465-482.
313. Wang, W.-m., et al., *Changes in composition, structure, and properties of jute fibers after chemical treatments*. Fibers and Polym., 2009. 10(6): p. 776-780.
314. Rojo, E., et al., *Comprehensive elucidation of the effect of residual lignin on the physical, barrier, mechanical and surface properties of nanocellulose films*. Green Chem., 2015. 17(3): p. 1853-1866.
315. Nair, S.S. and Yan, N.J.C., *Effect of high residual lignin on the thermal stability of nanofibrils and its enhanced mechanical performance in aqueous environments*. Cellulose, 2015. 22(5): p. 3137-3150.
316. Wei, L., et al., *Performance of high lignin content cellulose nanocrystals in poly (lactic acid)*. Polymer, 2018. 135: p. 305-313.
317. Peng, Y., et al., *Effects of lignin content on mechanical and thermal properties of polypropylene composites reinforced with micro particles of spray dried cellulose nanofibrils*. ACS Sustain. Chem. Eng., 2018. 6(8): p. 11078-11086.

318. Ferrer, A., et al., *Effect of residual lignin and heteropolysaccharides in nanofibrillar cellulose and nanopaper from wood fibers*. 2012. 19(6): p. 2179-2193.
319. Degrassi, G., Vindigni, A., and Venturi, V., *A thermostable α -arabinofuranosidase from xylanolytic bacillus pumilus: Purification and characterisation*. J. Biotechnol., 2003. 101(1): p. 69-79.
320. Lama, L., et al., *Purification and characterization of thermostable xylanase and β -xylosidase by the thermophilic bacterium bacillus thermantarcticus*. Microbiol. Res., 2004. 155(4): p. 283-289.
321. Orth, A.B., Royse, D., and Tien, M., *Ubiquity of lignin-degrading peroxidases among various wood-degrading fungi*. Appl. Environ. Microbiol., 1993. 59(12): p. 4017-4023.
322. Eggert, C., Temp, U., and Eriksson, K.-E.L., *Laccase is essential for lignin degradation by the white-rot fungus pycnoporus cinnabarinus*. FEBS Lett., 1997. 407(1): p. 89-92.
323. Rico, A., et al., *Pretreatment with laccase and a phenolic mediator degrades lignin and enhances saccharification of eucalyptus feedstock*. Biotechnol. Biofuels, 2014. 7(1): p. 6.
324. Murphy, C., et al., *Curation of characterized glycoside hydrolases of fungal origin*. Database, 2011. 2011.
325. Langston, J.A., et al., *Oxidoreductive cellulose depolymerization by the enzymes cellobiose dehydrogenase and glycoside hydrolase 61*. Appl. Environ. Microbiol., 2011. 77(19): p. 7007-7015.
326. Božič, M., et al., *Enzymatic phosphorylation of cellulose nanofibers to new highly-ions adsorbing, flame-retardant and hydroxyapatite-growth induced natural nanoparticles*. Cellulose, 2014. 21(4): p. 2713-2726.
327. Egusa, S., et al., *Surface modification of a solid-state cellulose matrix with lactose by a surfactant-enveloped enzyme in a nonaqueous medium*. J. Mater. Chem., 2009. 19(13): p. 1836-1842.
328. Božič, M., et al., *New findings about the lipase acetylation of nanofibrillated cellulose using acetic anhydride as acyl donor*. Carbohydr. Polym., 2015. 125: p. 340-351.
329. Xie, J. and Hsieh, Y.L., *Enzyme-catalyzed transesterification of vinyl esters on cellulose solids*. J. Polym. Sci. A, 2001. 39(11): p. 1931-1939.

List of Figures

Chapter I: Introduction

Figure 1.1. Cellulose chemical structure	10
Figure 1.2. Cellulose semi-crystalline structure	11
Figure 1.3. Cellulose polymorphs	12
Figure 1.4. Hierarchical cellulose structure	14
Figure 1.5. Nanocellulose types	15
Figure 1.6. Nanocellulose application	17
Figure 1.7. Polyurethane structure	18
Figure 1.8. Esterification reaction in cellulose by sulfuric acid hydrolysis	21
Figure 1.9. Ancestral sequence reconstruction	24
Figure 1.10. Enzymatic cellulose degradation by cellulases	25
Figure 1.11. LPMO catalytic activity	27
Figure 1.12. Lignocellulosic biomass	28
Figure 1.13. Xylanase catalytic reaction	29
Figure 1.14. Ancestral endoglucanase reconstruction	31
Figure 1.15. Ancestral xylanase and LPMO reconstruction	32

Chapter II: Materials and methods

Figure 2.1. pQE-80L expression plasmid	41
--	----

Figure 2.2. General protein and purification protocol	48
Figure 2.3. Nanocellulose isolation protocol	50
Figure 2.4. Lignocellulosic substrates	51
Figure 2.5. Atomic force microscopy.	54
Figure 2.6. FTIR spectrum from filter paper	55
Figure 2.7. X-ray diffractogram of filter paper	58
Figure 2.8. CP/MAS ^{13}C NMR spectra of cellulose	59
Figure 2.9. Weight loss with temperature (A) and DTG (B) curves from filter paper	60
Figure 2.10. WBPU synthesis scheme	62
Figure 2.11. WBPU/CNC nanocomposite	63
Figure 2.12. DSC thermogram from WBPU matrix	66
Figure 2.13. Water contact angle	68
Figure 2.14. Conductive nanopapers preparation	70
Chapter III: Nanocellulose isolation with ancestral endoglucanase	
Figure 3.1. Nanocellulose produced by ancestral endoglucanase hydrolysis for 24 hours	80
Figure 3.2. (A) Nanocellulose, (B) reducing sugars, and (C) total conversion from filter paper using ANC EG, ANC EG+CBM and from <i>T. maritima</i> EG at 50 °C	81
Figure 3.3. AFM images of nanoparticles produce by EGs	84

hydrolysis at different time points (5 μm x 5 μm)

Figure 3.4. AFM images of nanoparticles produced with 87
ancestral endoglucanase with CBM hydrolysis (A) (3 μm x 3
 μm) and sulfuric acid (B)

Figure 3.5. Size distribution of nanocellulose particles produced 88
with the (A) ANC EG, (B) ANC EG+CBM, and (C) *T. maritima*
EG

Figure 3.6. Comparison of size distribution of nanocellulose 89
produced with enzymatic hydrolysis and the ones produced
using sulfuric acid hydrolysis

Figure 3.7. FTIR spectra of nanocellulose produced by ANC EG 92
hydrolysis of filter paper at 1, 5, 24, 48 and 72 hours

Figure 3.8. FTIR spectra of nanocellulose produced by ANC 93
EG+CBM hydrolysis of filter paper at 1, 5, 24, 48 and 72 hours

Figure 3.9. Comparison of FTIR spectra of filter paper, sulfuric 93
acid hydrolysis produced nanocellulose, and nanocellulose
produced by ANC EG and ANC EG+CBM hydrolysis at 24
hours

Figure 3.10. Second derivative FTIR spectra of filter paper, 96
EnCNCs from hydrolysis with both ANC EGs and AcCNC

Figure 3.11. Spectra of nanocellulose particles produced by 5 97
hours hydrolysis of ANC EG+CBM measured by nano-FTIR

- Figure 3.12. Comparison of nanocellulose particles spectra 98
produced by ANC EG+CBM 5 hours hydrolysis measured with
ATR-FTIR versus the average spectrum measured with Nano-
FTIR
- Figure 3.13. Conductometric titration curve of cellulose 100
nanocrystals produced by sulfuric acid hydrolysis
- Figure 3.14. (A) Aqueous suspension of EnCNCs and AcCNCs. 101
(B) Illustration of free -OH groups in EnCNC surface and the
random -OSO₃⁻ groups anchored by the sulfuric acid treatment in
the AcCNC surface
- Figure 3.15. X-ray diffraction analysis of the filter paper, 101
EnCNCs produced by 24 hours hydrolysis of ANC EG and ANC
EG+CBM, and AcCNCs produced by sulfuric acid hydrolysis
- Figure 3.16. CP/MAS ¹³C NMR spectra of the filter paper, 106
EnCNCs produced by 24 hours hydrolysis of ANC EG and ANC
EG+CBM and AcCNC produced by sulfuric acid hydrolysis
- Figure 3.17. Thermogravimetric analysis curves of the filter 108
paper, EnCNCs produced by 24 hours hydrolysis of ANC EG,
and ANC EG+CBM and AcCNCs produced by sulfuric acid
hydrolysis
- Chapter IV: Nanocellulose isolation from
lignocellulosic biomass with enzymatic cocktail
- Figure 4.1. Nanocellulose on water suspension and freeze-dried 115

isolated from Bleached Kraft pulp (BKP) and Unbleached Kraft pulp (KAPPA)

Figure 4.2. (A) Nanocellulose, (B) reducing sugars and (C) total conversion from BKP and KAPPA using ancestral enzymes mixtures and query enzymes at 50 °C in 24 hours of hydrolysis 116

Figure 4.3. AFM images (3 μm x 3 μm) of nanocellulose from BKP and KAPPA using ancestral enzymes mixtures and query enzymes at 50 °C in 24 hours of hydrolysis 120

Figure 4.4. Size distribution of nanocellulose particles produced from BKP (A) and KAPPA (B) using ancestral enzymes mixtures and query enzymes at 50 °C in 24 hours of hydrolysis 122

Figure 4.5. FTIR spectra of nanocellulose produced from BKP using ancestral enzymes mixtures at 50 °C in 24 hours of hydrolysis 125

Figure 4.6. FTIR spectra of nanocellulose produced from KAPPA using ancestral enzymes mixtures at 50 °C in 24 hours of hydrolysis 126

Figure 4.7. Second derivative of FTIR spectra of nanocellulose produced from BKP using ancestral enzymes at 50 °C in 24 hours of hydrolysis 127

Figure 4.8. Second derivative of FTIR spectra of nanocellulose produced from KAPPA using ancestral enzymes mixtures at 50 °C in 24 hours of hydrolysis 128

Figure 4.9. X-ray diffraction of nanocellulose produced from BKP using ancestral enzymes mixtures at 50 °C in 24 hours of hydrolysis 130

Figure 4.10. X-ray diffraction analysis of nanocellulose produced from KAPPA using ancestral enzymes mixtures at 50 °C in 24 hours of hydrolysis 131

Figure 4.11. CP/MAS ^{13}C NMR spectra of nanocellulose produced from BKP using different enzymes mixtures at 50 °C in 24 hours of hydrolysis 133

Figure 4.12. CP/MAS ^{13}C NMR spectra of nanocellulose produced from KAPPA using different enzymes mixtures at 50°C in 24 hours of hydrolysis 134

Figure 4.13. Thermogravimetric analysis of nanocelluloses produced from BKP using different enzymes mixtures at 50 °C in 24 hours of hydrolysis 136

Figure 4.14. Thermogravimetric analysis of nanocelluloses produced from KAPPA using different enzyme mixtures at 50 °C in 24 hours of hydrolysis 137

Chapter V: Enzymatic nanocellulose applications

Figure 5.1. Photographs of WBPU matrix and nanocomposites with different concentrations, 1, 3, 5 and 7 wt% of EnCNC and AcCNC after casting and vacuum drying 143

Figure 5.2. AFM height and phase images (2 μm x 2 μm) of 145

WBPU matrix and WBPU nanocomposites with 5 wt% EnCNCs
and AcCNCs

Figure 5.3. SEM images from the cross section of WBPU matrix 146
and WBPU nanocomposites with different concentration of
EnCNC and AcCNC after cryo-facture

Figure 5.4. Comparison between FTIR spectra of WBPU matrix, 148
nanocomposites with different EnCNC concentrations and
EnCNC

Figure 5.5. Comparison between FTIR spectra of WBPU matrix, 149
nanocomposites with different AcCNC concentrations and
AcCNC

Figure 5.6. Second derivative analysis from FTIR spectra of 150
WBPU matrix, WBPU with 7 wt% EnCNC and AcCNC

Figure 5.7. Analysis of C=O groups absorption in the WBPU 151
nanocomposites

Figure 5.8. DSC thermograms of WBPU matrix and 152
nanocomposites with different concentrations of EnCNCs

Figure 5.9. DSC thermograms of WBPU matrix and 153
nanocomposites with different concentrations of AcCNCs

Figure 5.10. Weight loss (A) and DTG curves (B) of WBPU 157
matrix, polyol and nanocomposites prepared with different
EnCNC concentrations

Figure 5.11. Weight loss (A) and DTG curves (B) of WBPU matrix, polyol and nanocomposites prepared with different AcCNC concentrations	158
Figure 5.12. DTG curves of WBPU matrix and nanocomposites with 7 wt% of both CNCs	159
Figure 5.13. Storage modulus and $\text{Tan}\delta$ of WBPU matrix and nanocomposites with different concentrations of EnCNCs	161
Figure 5.14. Storage modulus and $\text{Tan}\delta$ of WBPU matrix and nanocomposites with different concentrations of AcCNCs	162
Figure 5.15. Storage modulus and $\text{Tan}\delta$ of WBPU matrix and nanocomposites with 7 wt% concentration of EnCNC and AcCNC	163
Figure 5.16. Stress-strain curves of WBPU matrix and nanocomposites with different concentrations of EnCNC and AcCNC.	165
Figure 5.17. Young's modulus of WBPU matrix and nanocomposites with different concentrations of EnCNC and AcCNCs	166
Figure 5.18. Contact angle of water drop over WBPU matrix and nanocomposites with different concentration of EnCNC and AcCNCs	168
Figure 5.19. Photographs of EnCNC and AcCNC films.	170

Figure 5.20. EnCNC film and AcCNC film immersed in water for three minutes	170
Figure 5.21. SEM images of EnCNC and AcCNC films at different magnifications	171
Figure 5.22. Photographs of films prepared with EnCNC and EnCNC films with different reduced graphene content: 2, 5, and 10 wt%	172
Figure 5.23. AFM images of graphene oxide suspension	173
Figure 5.24. SEM images of films prepared with EnCNC and EnCNC with different graphene content: 2, 5, and 10 wt%	174
Figure 5.25. Magnified of SEM images of EnCNC film with 10 wt% content of reduced graphene	175
Figure 5.26. Comparison of FTIR spectra of GO, rGO, EnCNC films with different rGO concentrations and EnCNC	176
Figure 5.27. Second derivative analysis from FTIR spectra of EnCNC film and EnCNC film with 10% rGO	178
Figure 5.28. Young's Modulus of the EnCNC film and EnCNC films with different rGO concentrations	179
Figure 5.29. Stress-strain curves of EnCNC films and EnCNC films with different rGO concentrations	181
Figure 5.30. Weight loss (A) and DTG curves (B) of EnCNC	182

film and the EnCNC films with different rGO content

Figure 5.31. Water contact angle measurement for neat EnCNC 184
and nanocomposites with different rGO content

Figure 5.32. Conductive properties of EnCNC films with 185
different rGO content

Figure 5.33. EnCNC film with CVD graphene film 187

Chapter VI: Discussion

Fig 6.1. Depending on the source, the enzymatic treatment and 197
the hydrolysis time, we can produce several nanocellulose
products adapted to the desired application. We can isolate high
pure or oxidized nanocellulose, both CNF and CNCs or even
nanocellulose with lignin residues

List of Tables

Chapter I: Introduction

Table 1.1. Examples of length and diameter of CNC produced with different treatments from several sources 20

Chapter III: Nanocellulose isolation with ancestral endoglucanase

Table 3.1. Average length, diameter and L/D aspect ratio of the nanocellulose produced at different hydrolysis times with ANC EG, ANC EG+CBM and *T. maritima* EG using filter paper as a substrate, and AcCNC. 86

Table 3.2. Crystallinity index (CI%) and crystallite size of the filter paper, EnCNCs produced by 24 hours hydrolysis of ANC EG and ANC EG-CBM and AcCNCs produced by sulfuric acid hydrolysis 104

Table 3.3. Onset degradation temperature (T_o), maximum thermal degradation temperature (T_d) and char residue (%) of the filter paper, EnCNCs produced by 24 hours hydrolysis of ANC EG and ANC EG+CBM, and AcCNCs produced by sulfuric acid hydrolysis 110

Chapter IV: Nanocellulose isolation from lignocellulosic

biomass with enzymatic cocktail

Table 4.1. Average length, diameter and L/D aspect ratio of the nanocellulose produced from BKP and KAPPA using ancestral enzymes mixtures and query enzymes at 50°C in 24 hours of hydrolysis 121

Table 4.2. Crystallinity index (CI%) and crystallite size of nanocellulose produced from BKP and KAPPA using different enzymes mixtures for 24 hours hydrolysis at 50 °C 132

Table 4.3. Onset degradation temperature (To), maximum thermal degradation temperature (Td) and the residue of the nanocellulose produced from BKP and KAPPA using different enzymes mixtures at 50 °C in 24 hours of hydrolysis 138

Chapter V: Enzymatic nanocellulose applications

Table 5.1. Thermal properties of WBPU matrix and nanocomposites with different EnCNC and AcCNC content 155

Table 5.2. Onset degradation temperature (To), thermal degradation of urea groups (Td₁), thermal degradation of urethane groups (Td₂), thermal degradation of soft segment (Td₃) and char residue from WBPU matrix and nanocomposites with different EnCNC and AcCNC content 160

Table 5.3. Storage modulus at 20 °C and Tanδ peak temperature (Tg_{SS}) of WBPU matrix and nanocomposites with different 164

concentrations of EnCNC and AcCNCs

Table 5.4. Mechanical properties of WBPU matrix and 167
nanocomposites with different concentrations of EnCNC and
AcCNCs

Table 5.5. Mechanical properties of EnCNC film and EnCNC 180
films with different rGO concentrations

Table 5.6. Thermal properties of EnCNC film and EnCNC films 183
with different rGO concentrations

Table 5.7. Comparison of conductive properties of EnCNC films 186
with reduced graphene

List of Abbreviations

AcCNC: Nanocrystals prepared by sulfuric acid treatment

AFM: Atomic force microscopy

ANC EG: Ancestral Endoglucanase

ANC EG+CBM: Ancestral endoglucanase with Carbohydrate Binding Module attached

ANC LPMO: Ancestral lytic polysaccharide monooxygenase

ANC XLN: Ancestral xylanase

B. subtilis: *Bacillus subtilis*

BC: Bacterial cellulose

BG: β -glucosidase

BglS: *Bacillus subtilis* Endoglucanase

BKP: Bleached Kraft pulp

CBH: Exoglucanase

CBM: Carbohydrate-Binding Module

CI%: Crystallinity index

CNC: Cellulose nanocrystals

CNF: Cellulose nanofibers

CP/MAS ^{13}C NMR: Cross-polarization magic angle spinning ^{13}C nuclear magnetic resonance

CTE: Coefficient of thermal expansion

CVD: Chemical vapour deposition

DBTDL: Dibutyltin dilaurate

DMA: Dynamic mechanical analysis

DMPA: 2,2-bis (hydroxymethyl) propionic acid

DNA: Deoxyribonucleic acid

DNS: 3,5-dinitrosalicylic acid

DSC: Differential scanning calorimetry

DTG: Derivative of thermogravimetric curve

E. coli: *Escherichia coli*

EDA: Ethylene diamine

EG: Endoglucanase

EnCNC: Enzymatic produced nanocrystals

FTIR: Fourier-transform infrared spectroscopy

GO: graphene oxide

HS: Hard segment

IPDI: Isophorone diisocyanate

IPTG: Isopropyl β -D-1-thiogalactopyranoside

IR s-SNOM: Scattering-type scanning near-field optical microscopy

IR: infrared

KAPPA: Unbleached Kraft pulp

LPMO: Lytic polysaccharide monooxygenases

MW: Molecular weight

Nano-FTIR: Nanoscale-resolved Fourier transform infrared

OD: Optical density

PC: Polycarbonate

PET: Polyethylene terephthalate

PLA: Polylactic acid

PMMA: Poly (methyl methacrylate)

PVA: Polyvinyl alcohol

rGO: Reduced graphene oxide

S. viridosporus: *Streptomyces viridosporus*

SEM: Scanning electron microscopy

SS: Soft segment

T. maritima: *Thermotoga maritima*

TEA: Triethylamine

TEMPO: 2,2,6,6-Tetramethylpiperidine-1-oxyl

TGA: Thermogravimetric analysis

WBPU: Waterborne polyurethane

XLN: Xylanase

XRD: X-ray diffraction

List of Symbols

E' : Stage modulus

I_{200} : Intensity of crystalline peak

I_{am} : Intensity of amorphous peak

L/D : Length/diameter

q : Specific resistance

R_s : Sheet resistance

t : Thickness

$\tan\delta$: Tangent of phase angle

T_d : Maximum degradation temperature

T_{gSS} : Glass transition temperature from the soft segment

T_{HS} : Hard segment short range order transition

T_{mSS} : Melting temperature from the soft segment

T_o : Temperature of the loss of 5% of the weight of the total sample

β : Full-width at half maximum of the (200) peak

ΔH_{HS} : Enthalpy of hard segment short range order transition

θ : Angle of the (200) plane

θ_c : Contac angle

κ : Constant value from XRD

λ : Wavelength of the incident X-ray

τ : Crystallite size

ω : Weight of AcCNC in conductometry titration.

